UNIVERSITY OF CALIFORNIA SAN DIEGO

Biochemical Analysis of Ribosome-associated E3 Ligase ZNF598 Functional Domains

A Thesis submitted in partial satisfaction of
the requirements for the degree Master of Science

in

Biology

by

Ruoyu Li

Committee in charge:

Professor Eric J. Bennett, Chair
Professor Jens Lykke-Anderson
Professor Randy Hampton

2018

The Thesis of Ruoyu Li is approved, and it is acceptable in quality and form for publication on microfilm and electronically:

_____

_____

_____

_____

Chair

University of California San Diego

2018

TABLE OF CONTENTS

LIST OF FIGURES

ACKNOWLEDGEMENTS

I would like to acknowledge Professor Eric Bennett for his support as a mentor and as the chair of my committee. Thank you for always being encouraging, patient and supportive at this early onset of my research journey.

I would like to thank Elayanambi Sundaramoorthy who served as my direct mentor in lab and also had contributed tremendously as the co-author of this thesis work. I appreciate your training in both laboratory techniques and critical thinking skills. I see you not only as an excellent researcher who I wish to become one day but also a role model in life as you are always calming, humble and helpful to everyone.

I would also like to thank Danielle Garshott, who is another graduate student in the lab and the entire Bennett lab for nurturing me not only with a wide breadth of scientific knowledge but also providing me with a loving home.

In the end, I would like to especially thank my parents as they had sacrificed so much ever since I came to the U.S. I will always keep your words in mind wherever I go.

This whole thesis will be prepared for submission for publication of the material. Li, Ruoyu; Sundaramoorthy, Elayanambi. The thesis authors are the primary investigators and the authors of the materials.

ABSTRACT OF THE THESIS

Biochemical Analysis of Ribosome-associated E3 Ligase ZNF598 Functional Domains

by

Ruoyu Li

Master of Science in Biology

University of California San Diego, 2018

Professor Eric J. Bennett, Chair

Premature mRNA polyadenylation, stop codon loss, or stop codon read-through results in decoding of poly(A) sequences which is a signal to induce ribosome-associated quality control events. ZNF598 is an important mammalian ribosome-associated E3 ligase that is involved in resolving stalled ribosomes attempting to translate poly(A)-containing sequences. ZNF598 regulates stall resolution via its ubiquitylation of two ribosomal proteins: RPS10 and RPS20. Our biochemical analysis of ZNF598 N-terminal domain truncations identifies the critical zinc fingers that are required for RPS10 and RPS20 ubiquitylation. Our results demonstrate that 1) RPS10 and RPS20 ubiquitylation, on their own, is insufficient to mediate proper ribosome stall resolution; 2) RPS10 and RPS20 ubiquitylation specificity depends on the length of the N-terminal region of ZNF598; 3) the N-terminal functional domains of ZNF598 are necessary but insufficient to trigger the poly(A)-induced stalling event.

Chapter1: Introduction

Ribosomes are molecular machines made up of 80 proteins and 4 RNAs (in mammals/higher eukaryotes), harboring the catalytic ensemble that orchestrates the faithful decoding of mRNA to their cognate polypeptide (Nicholson and Mühlemann, 2010). Nearly 200 assembly factors, chaperones , and RNA manipulating proteins ensure production of functional ribosomes (Pena, Hurt et al. 2017). Several proteins interact with the mature ribosome in the cytoplasm(Fleischer, Weaver et al. 2006) and regulate several novel aspects of regulated translation. A recent mass spectrometry based proteomic survey of this interactome identified approximately 430 proteins in mouse embryonic stem cells (Simsek, Tiu et al., 2017). Several of the interactors regulate translation(Simsek, Tiu et al., 2017) through direct binding to mRNA elements (Ascano, Mukherjee et al., 2012) or to the ribosome (Shao, Brown et al., 2015) and regulate dynamic post-translational modifications of ribosomal subunits(Simsek and Barna 2017). Under diverse stress conditions, cells adjust protein synthesis and degradation rates to maintain homeostasis (Harper and Bennett, 2016). Upon unfolded protein response (UPR) induction, upregulated PERK signaling will phosphorylate translation initiation factor α, eIF2α, which results in the reduced the number of functional ternary complexes for translational initiation (Higgins et al., 2015). Moreover, UPR also triggers regulatory ribosomal ubiquitylation (RRub) on 40S subunit. Both PERK and RRub protect cells from UPR-stimulated cell death by reducing translation (Higgins et al., 2015). While several kinase signaling cascades that regulate ribosomes have been known (Meyuhas, 2015), the role of ubiquitylation as a dynamic post-translational modification, akin to phosphorylation, is emerging (Higgins, Gendron et al., 2015; Silva, Finley et al., 2015).

Genetic screens performed in yeast to identify regulators of heat shock response transcription factor Hsf1 or the ski helicase complex, identified a ribosome-associated protein complex that was termed the ribosome quality control complex (RQC)(Brandman, Stewart-Ornstein et al., 2012; Defenouillere, Yao et al., 2013). RQC factors are involved in the elimination of polypeptides generated from mRNAs that lack a stop codon, a substrate for the non-stop mRNA decay (NSD) pathway(Joazeiro, 2017). Several proteasome components and chemical inhibitors of the proteasome were identified as pathway components in these genetic screens (Ito-Harashima, Kuroha et al., 2007). Among them, the ribosome-associated protein quality control (RQC) system stands out, as it surveils protein synthesis by preventing the faulty translational products at the "factory site" – ribosomes, detecting and resolving the error-prone "assembly lines" –the aberrant mRNAs, and destroying the problematic products, which are the nascent peptide chains. The following section outlines this pathway and its components.

1.1 Factors that trigger terminal ribosome stalls during elongation

Translating ribosomes can encounter sudden pausing under several contexts such as secreted protein synthesis, mediated by signal recognition particle induced forced stall (Richter and Coller, 2015), mRNAs with repetitive rare codons and unique codon adjacency (Brule and Grayhack, 2017). Several of these are physiologically regulated and do not engage the RQC machinery. Whereas the mRNA specific deficiencies listed below regulate the fate of the mRNA, the nascent protein and the ribosome and in certain scenarios engage the RQC pathway. In a cell with robust RQC, the ribosomes respond to reading the aberrant mRNA with recruitment of appropriate RQC complexes, commonly seen with mRNAs with chemical damage or mRNAs that have been subjected to endonuclease digestion(Joazeiro, 2017). The three main categories of

aberrant mRNA decay are: No-go decay (NGD) and nonsense-mediated decay (NMD), which are usually caused by transcripts with obstacles during elongation, as well as the Non-stop decay (NSD), which is a result of truncated mRNAs lacking a stop codon or stop codon readthrough events (Figure 1). All three mRNA defects will trigger ribosomal stalling, and subsequent steps of ribosome subunit rescue, mRNA decay and protein degradation varies in each situation(Lykke-Andersen and Bennett, 2014).

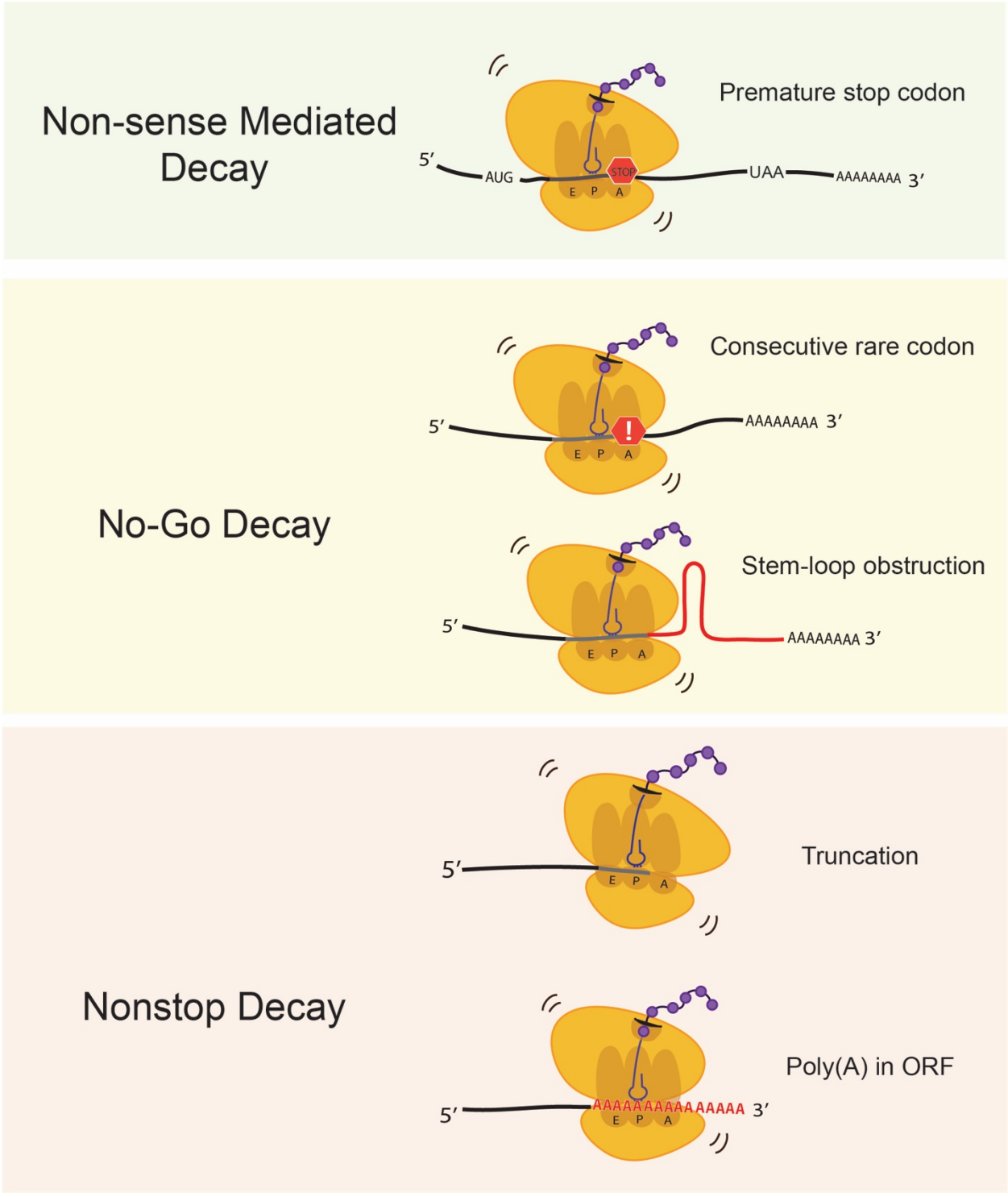

Figure 1. Distinct mRNA Decay pathways
Fives mRNA defects that can lead to ribosomal stalling are listed
The stalling situations initiate three types of mRNA decay pathways: Non-sense mediated decay, No-Go decay, and Nonstop decay.
E: exit site; P: peptidyl site; A: aminoacyl site.

During the normal translational cycle, aminoacyl-tRNA is brought to the A site based on the codon present within the A site by Elongation factor 1A (EF1A). GTP hydrolysis by EF1A accommodates the tRNA into the A site which is followed by peptide bond formation between the incoming amino acid and the polypeptide associated in the P site. Now, the polypeptide chain is in the A site, anchored by the new amino acid-tRNA. Subsequently, another GTPase Elongation Factor 2(EF2) is recruited to ribosome and catalyzes the translocation of A site polypeptide-tRNA into P site as well as the previous P site tRNA into the E site for release.

At the end of protein synthesis, a stop-codon occupancy in the A site of the ribosome signals for translation termination (Figure 2). In eukaryotes, eukaryote release factor 1 (eRF1) and eukaryote release factor 3 (eRF3) together form a GTP-dependent termination machinery (Mugnier and Tuite,1999). eRF1 then recruit AAA ATPase Rli1(in yeast)/ABCE (in mammals), which facilitates tRNA-peptidyl hydrolysis and also splits ribosomal subunits for recycling (Dever and Green, 2012) (Figure 2).

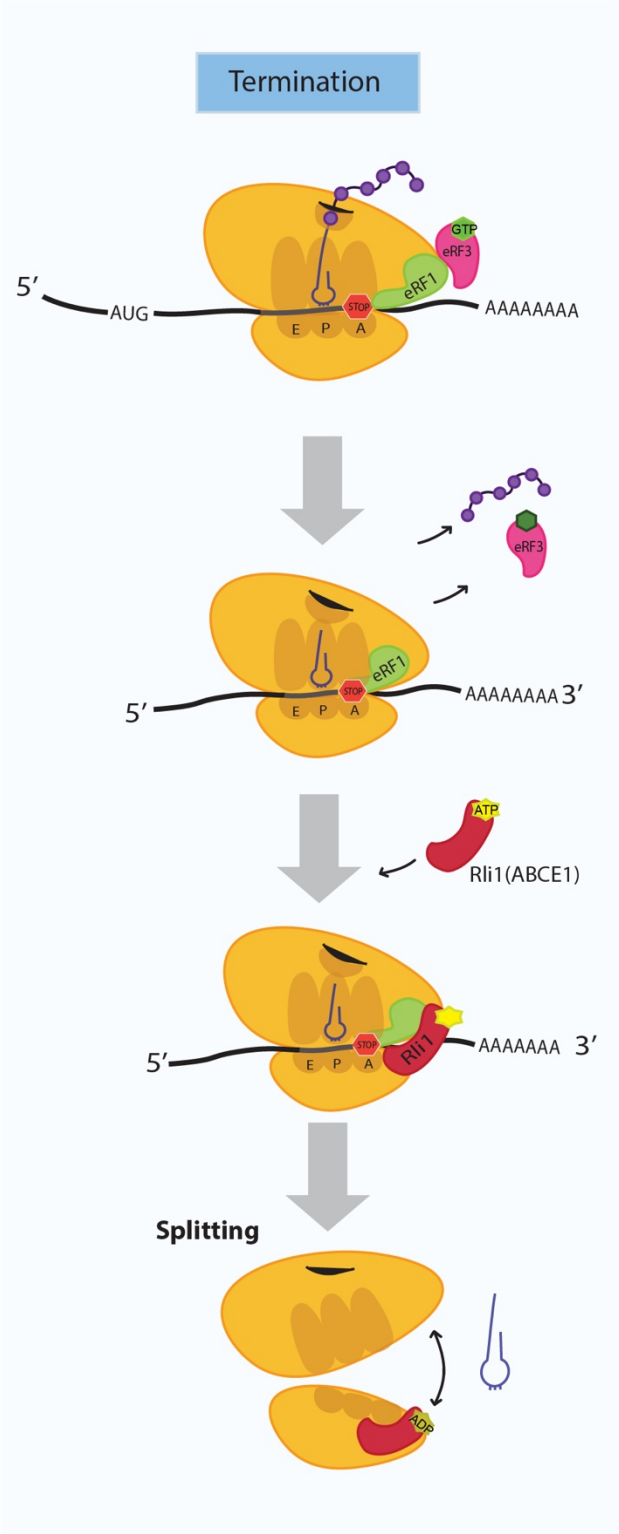

Figure 2. Normal Termination
E: exit site;
P: peptidyl site;
A: aminoacyl site.

1.1.1 Non-sense mediated decay (NMD)

NMD is triggered by a non-sense mutation resulting in a premature stop codon in an open reading frame (ORF) (Figure 3). NMD mRNA recruits Upf1, an ATP- dependent RNA helicase which is regulated by a group of SMG proteins for the downstream deadenylation and decapping of the mRNA (Nicholson and Muhlemann, 2010). It has been shown in many studies that deadenylation of NMD mRNA follows the conventional mRNA turnover pathway: starting with the removal of poly-(A) tails by Ccr4p-Caf1p complex decapping (in mammals this is mediated by the PAN2-PAN3 poly-A nuclease complex), followed by degradation by DCP2 (decapping enzyme 2), XRN1(5' to 3') and exosome-complex (3'to 5') (Nicholson and Muhlemann, 2010).

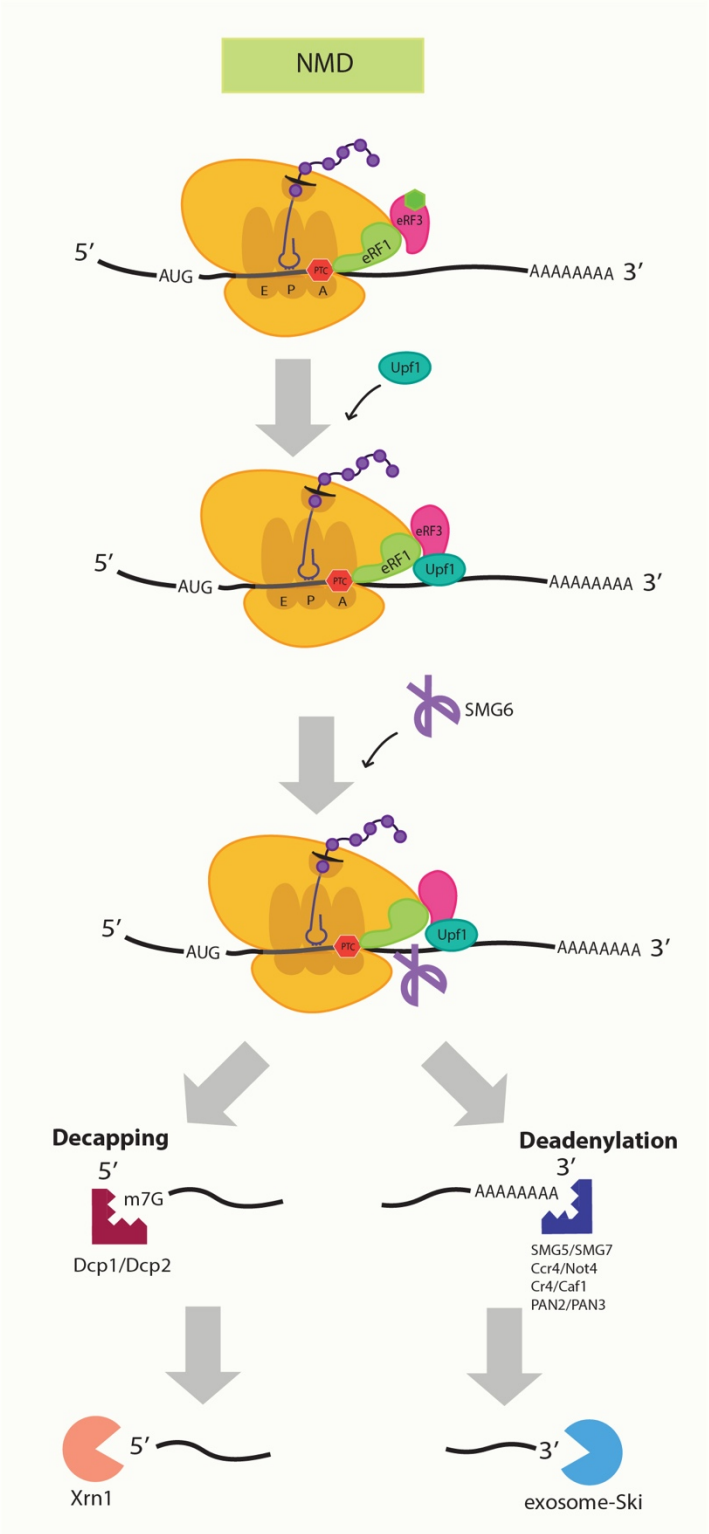

Figure 3. Non-sense Mediated Decay (NMD)
PTC: premature termination codon

1.1.2 No-Go Decay (NGD)

In the NGD pathway, mRNA's that stalls the ribosome either by structural inhibition through stable stem loop RNA structure or by introducing consecutive rare codons (Doma and Parker, 2006) initiates ribosome-associated quality control pathways (Figure 4). A stem loop forms a secondary structure in mRNA and prevents the ribosome from reading towards the 3' direction. As the leading ribosome encounters the translational obstacle and arrests, the ribosomes that follow will collide and form a stacked array. This ribosomal stacking event has been shown to trigger the endonucleolytic cleavage, by an as yet uncharacterized endo-ribonuclease(Simms, Yan et al., 2017). In yeast, the cleaved mRNA products will either undergo decapping and 5' to 3'degradation by a major exonuclease Xrn1, or deadenylation and 3' to 5' degradation by Exosome-Ski complex (Doma and Parker, 2006).

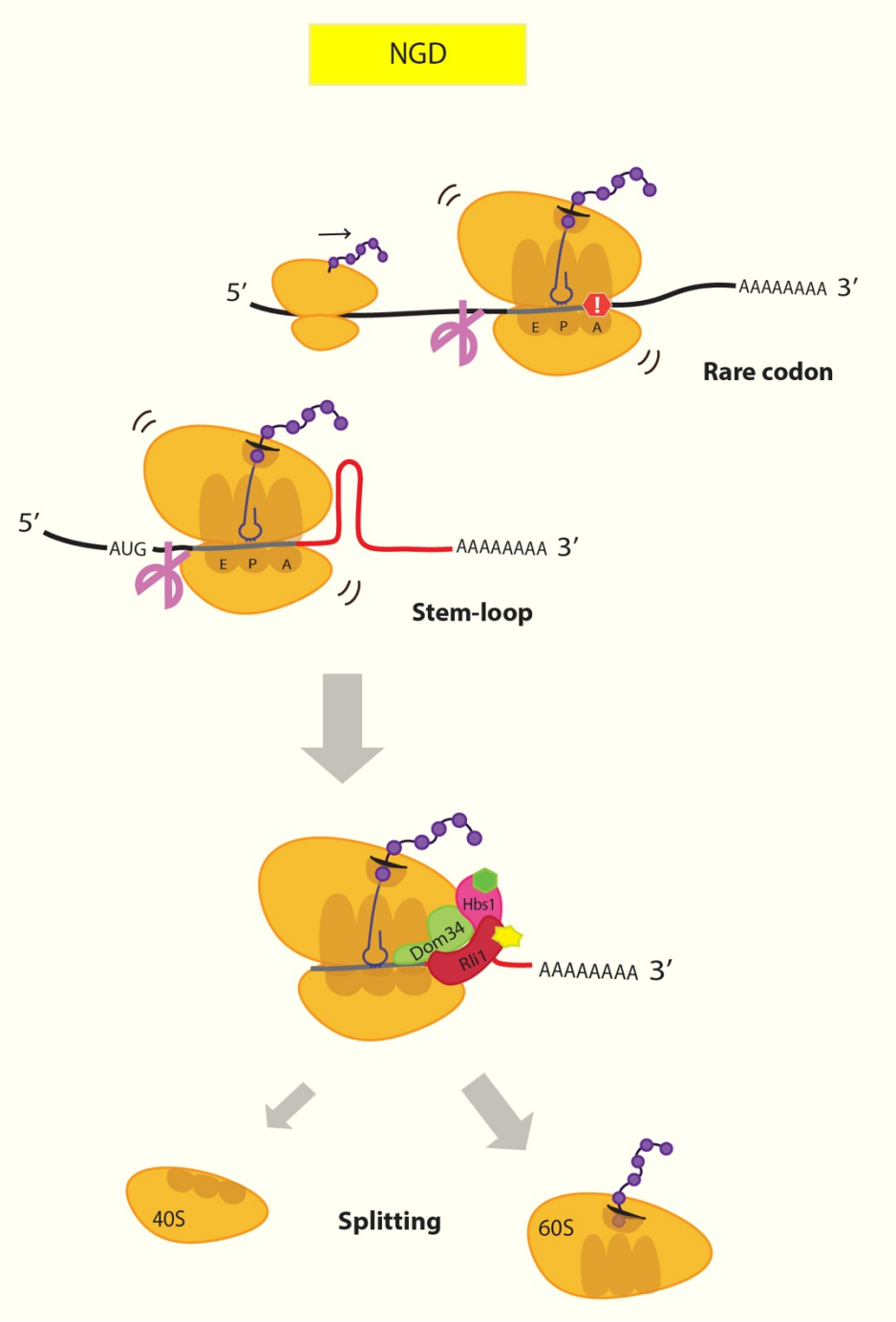

Figure 4. No-Go Decay (NGD)

1.1.3 Non-stop Decay (NSD)

Non-stop mRNA decay is characterized by aberrant transcripts that either lack a stop-codon or are polyadenylated in ORFs by premature polyadenylation. NSD mRNAs are classified into two types: Transcript I—in which truncations happen within the ORF, and Transcript II, which has loss-of-stop codon (Figure 5). Transcript I may arise from the 3'-end cleaved products generated in the NGD pathway (Joazeiro, 2017). Because these truncations happen in the ORFs, deadenylation is not needed prior to degradation, which separates NSD from the canonical RNA decay pathway, in which deadenylation has to take place before 3' degradation by Exosome-Ski complex (Klauer and van Hoof, 2012).

The premature polyadenylation that results into NSD Transcript II naturally occur at a frequency of 5% in yeast cells, and at 1% in mammalian cells (Ozsolak et al., 2010). Ribosome profiling approaches that combines ribosome footprinting and deep sequencing of the ribosome-associated mRNA renders a pause-site map during translation. Codon analysis of the short footprints, as a result of endonucleolytic cleavage, indicates the enrichment of the premature polyadenylation sequences associated with stalled ribosome (Guydosh and Green, 2017).

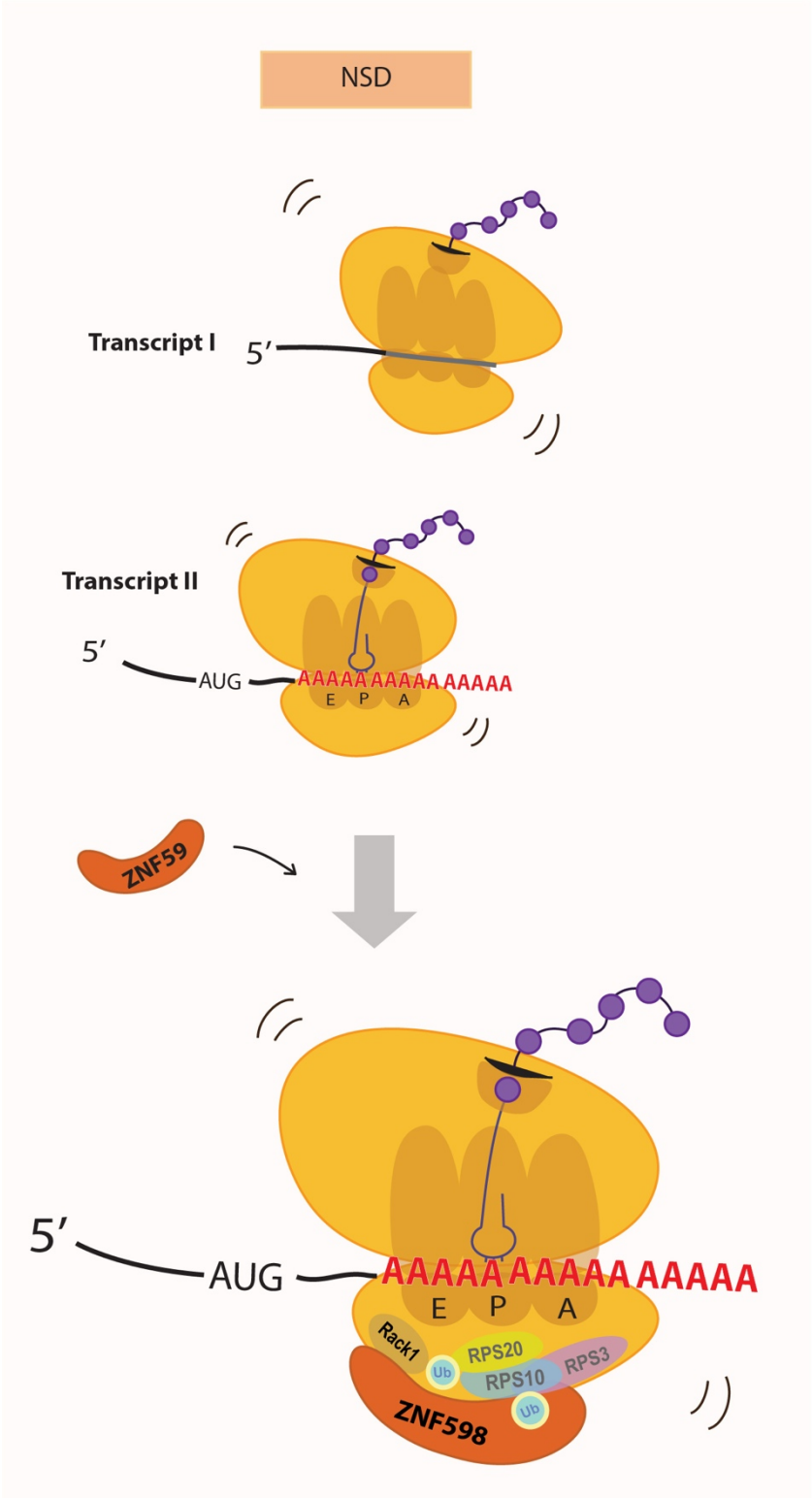

Figure 5. Nonstop Decay (NSD)

1.2 RQC FACTORS

1.2.1 Initial RQC Sensor: ZNF598/Hel2

Hel2, a RING domain E3 ligase, was first characterized in yeast to regulate translation of poly-basic sequence (Brandman et al., 2012). Its mammalian homolog, ZNF598 was also found to play a similar role in regulating nonstop mRNA translation: in the presence of ZNF598, ribosomes reading the poly-(A) sequence are forced into stalling thus activating the RQC pathway; however, in the absence of ZNF598 functionality, the ribosomes continue to translate the poly-(A) sequences into poly-lysine residues on the nascent chains and read into the post-stall sequences, which is termed as a "read-through" event (Figure 6a). Harnessing the stall-inducing potential of the poly-(A) sequence, a dual-fluorescence reporter, consisting of an upstream GFP protein, a stretch of poly-(A) sequence in the middle, and a downstream mCherry protein, is widely used to monitor the Nonstop translational stalls (Brandman 2012, Juszkiewicz and Hegde, 2017; Sundaramoorthy et al., 2017). These readthrough events were further confirmed in later studies utilizing the dual-fluorescent reporter as mentioned earlier, specifically in cell lines lacking ZNF598 protein product or its E3 ligase functionality (Sundaramoorthy et al., 2017). In addition, both Hel2 and ZNF598 have been found to associated with 80S ribosomal fractions in sucrose gradient, indicating that they bind to the ribosome prior to subunit splitting (Juszkiewicz and Hegde, 2017; Sitron et al., 2017; Sundaramoorthy et al., 2017).

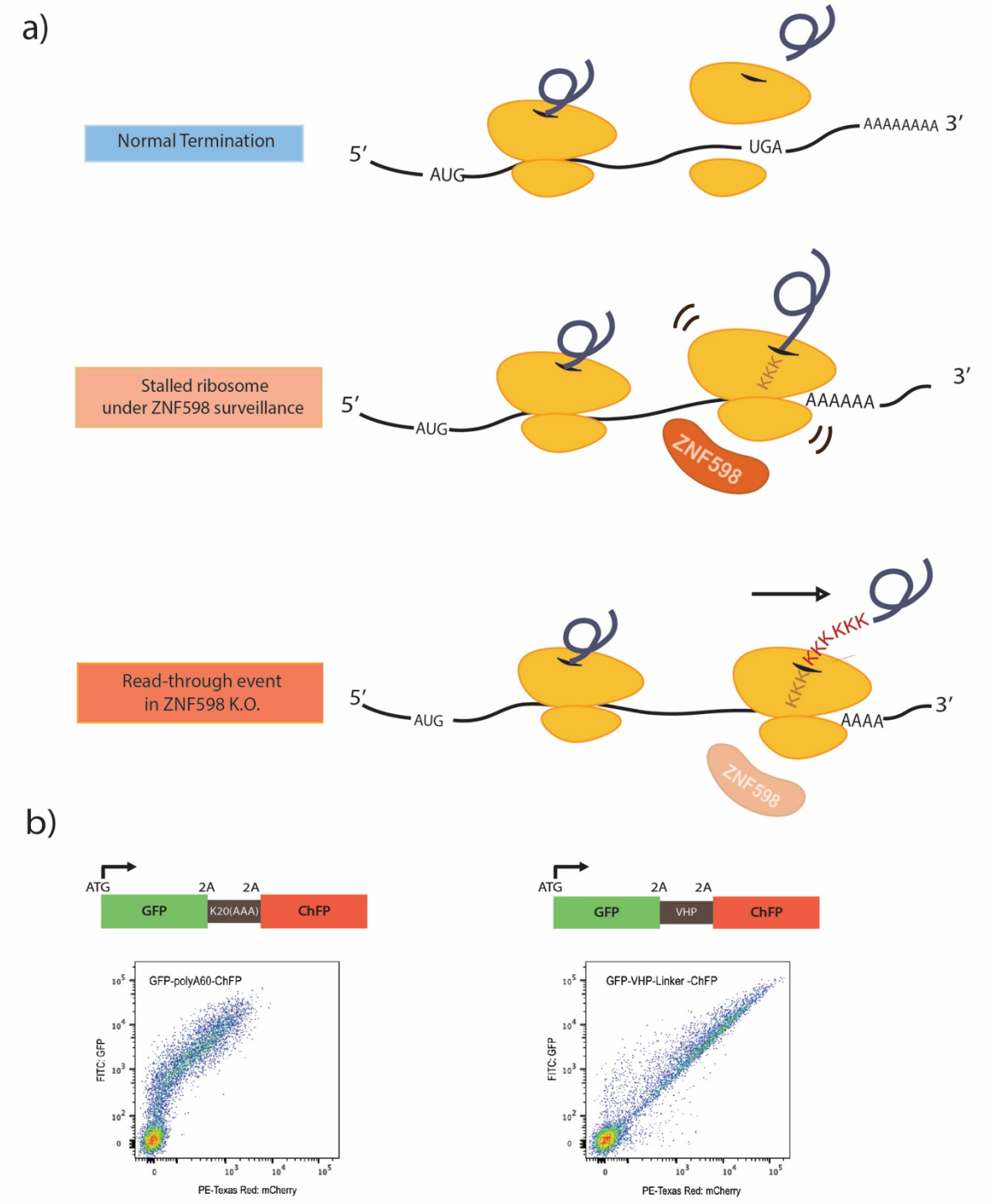

Figure 6. ZNF598/Hel2 RQC Surveillance and Dual Fluorescence Reporter Assay
a) comparison of normal termination, poly(A) surveillance with and without ZNF598
b) dual fluorescence reporter constructs and corresponding FACS plots

1.2.2 Post-splitting RQC on 60S: LTN1-associated Complexes

After splitting by Dom34-Hbs1-Rli1 complex in yeast, Ltn1(Listerin in mammals) directly targets the peptidyl-tRNA-bound 60S ribosomal subunit, to ubiquitylate the associated nascent chain. The Ltn1-mediated nascent chain ubiquitylation together with Rqc1 (TCF25 in mammals) recruit Cdc48 (VCP/p97 in mammals), which is an AAA ATPase that extracts the nascent chain for proteasomal degradation (Figure 7). In addition, Rqc2, another player in the Ltn1 RQC complex, stabilizes one end of Ltn1 to the 60S ribosomal subunit interface after splitting had occurred. Meanwhile, Rqc2's occupancy at the subunit interface prevents 40S re-association with the 60S, and it also modifies the nascent chain with non-templated C-terminus Alanine-Threonine tail (CAT-tail) that promotes nascent chain aggregation (Defenouillère et al., 2016).

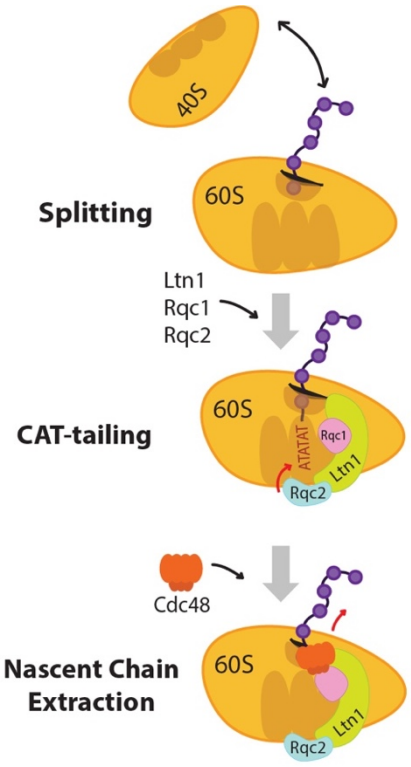

Figure 7. RQC on 60S: Ltn1-associated Complexes

1.3 UPS in Protein Degradation

Ubiquitin proteasome system (UPS) and autophagy-lysosome system are the two common protein degradation pathways system in eukaryotes. In general, the UPS is the first line of defense. A failed rescue by UPS would then initiate the pro-apoptotic autophagy-lysosomal pathway due to the overload defective proteins that cannot be cleared efficiently.

In the UPS, ubiquitylated substrates, mostly soluble proteins, are transported in the cytoplasm to the degradation machinery—proteasomes. Upon the arrival of substrates, the proteasome 19S cap complex recognizes the substrate-shuttling proteins and deubiquitylates the substrates for entry into the 20S complex. After the unfolded peptide chain enters the 20S proteolytic inner cores, peptidases degrade the substrates into short peptides that are subsequently fully trimmed to individual amino acids that can be recycled into the translation reaction. (Korolchuk et al., 2009) (Figure 8).

1.4 Ubiquitin biology

Ubiquitylation is a process in which one or a chain of ubiquitin proteins are added to protein substrates. Canonical ubiquitylation is achieved by a series of enzymatic reactions, in order, through ubiquitin activating enzyme (E1), ubiquitin conjugating enzyme (E2), and ubiquitin ligase (E3) (Figure 8). E1's activation of ubiquitin, an ATP-driven process, forms a thioester bond between C-terminus of ubiquitin and a catalytic Cys residue on E1. Next, the E1~Ub complex, transfers the ubiquitin to the Cys residue of a E2 enzyme through transthioesterification (Schulman and Harper, 2009). A typical E3 participates in the final step of ubiquitylating a substrate as it possesses an E2 binding domain and a substrate-recruiting domain, altogether bringing E2~ub and the substrate in proximity (Komander and Rape, 2012).

Once the ubiquitin gets transferred to the substrate, the discharged E2 will then disassociate from E3 allowing another Ub~E2 to bind. Putatively, there are two ubiquitin E1 enzymes, around 40 E2 enzymes, and 500-1,000 different E3 enzymes (Nakayama and Nakayama, 2006; Ye and Rape, 2009). The E2 enzymes supply ubiquitin to the E3 while the E3 determines the substrate specificity (Komander and Rape, 2012).

The covalently attached ubiquitin connects to the substrate with an isopeptide bond between the C-terminual glycine residue on ubiquitin and a lysine residue on the substrate. Multiple rounds of E2-Ub loading onto a substrate engaged ubiquitin ligase result in poly-ubiquitylation. How the lysine position alters upon Ub addition determines the structure of the chains—branched, mixed or homogenously extended (Komander and Rape, 2012). There are total 8 linkage sites on an ubiquitin protein: Met1, Lys11, Lys48, Lys63, Lys6, Lys27, Lys29, and Lys33. At a simple glance, the two most studied Lys-linkage chains: Lys63-linked and Lys48-linked are mainly involved in non-proteolytic and proteolytic pathways, respectively (Komander and Rape, 2012). However, more studies later had discovered that ubiquitin coding is more complex than that: different combinations of substrate ubiquitylation sites and ubiquitin chain topology write distinct fates of the substrates. (Komander and Rape, 2012).

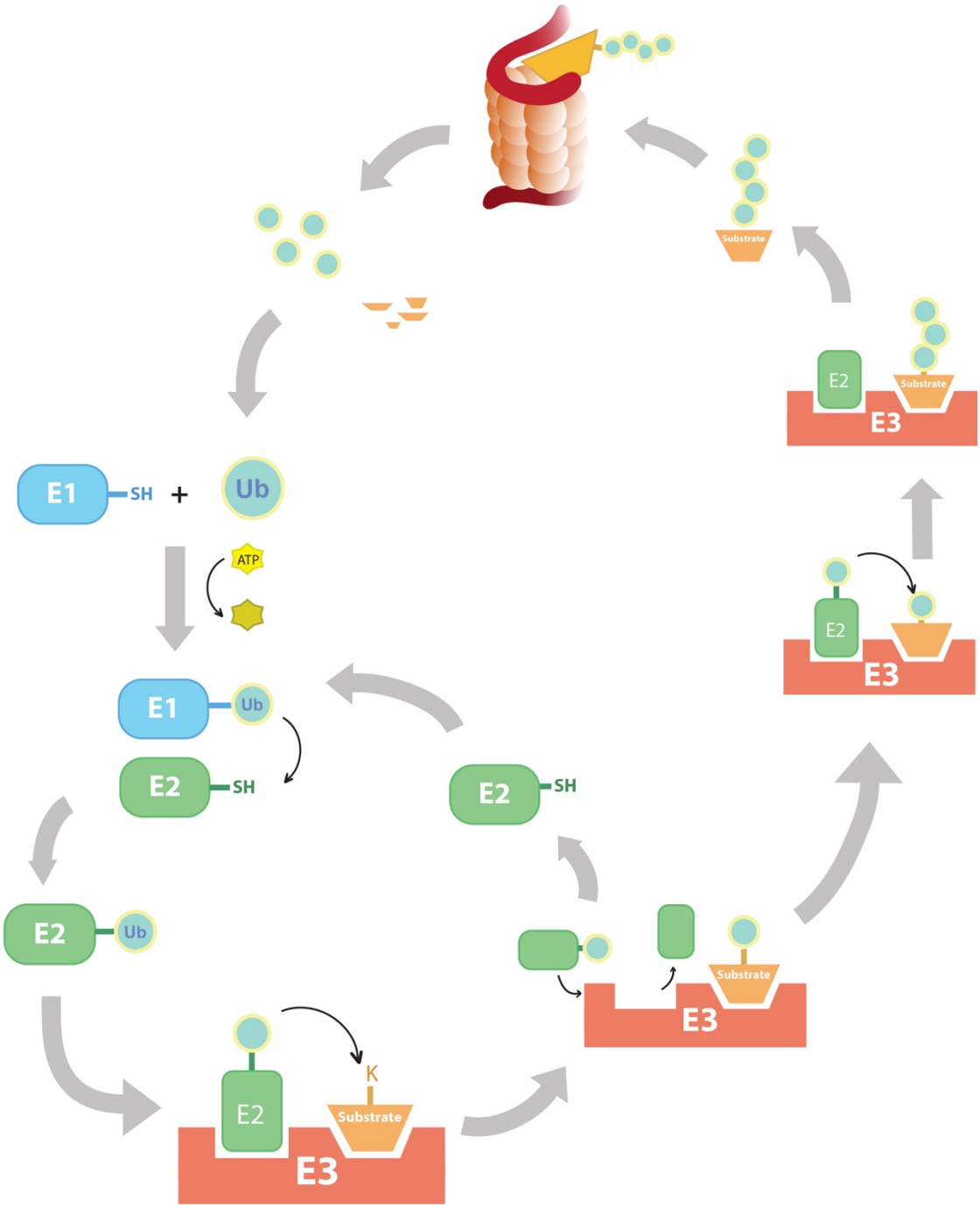

Figure 8. Ubiquitin Proteasome System (UPS)
-SH: Cysteine residue
-K: Lysine residue

1.5 RING Domain E3 ligase

E3 ligases in eukaryotes are classified by their domain architecture: containing either HECT (Homologous to E6-AP Carboxy Terminus)-domain or RING (Really Interesting New Gene)-domains. A HECT E3 ligase relays a ubiquitin from E2 via its Cys residue in the HECT domain before transferring to the substrate or to another ubiquitin. In contrast to HECT-domain E3s, in which a thioester bond is formed between the E3 and ubiquitin, RING E3s recruits ubiquitin-loaded E2s through its RING domain and catalyzes the direct Ub-transfer from E2 onto the substrate (Deshaies and Joazeiro, 2009) (Figure 9). The canonical RING domain sequence is described as Cys-X2 -Cys-X(9-39) -Cys-X(1-3) -His- X(2-3) -Cys-X2 -Cys-X(4-48) -Cys-X2 -Cys (X is any amino acid) (Borden and Freemont, 1996). Structural analysis reveals that RING domains coordinate two zinc atoms with cysteine and histidine residues, forming a hydrophobic core for protein-protein interaction (Deshaies and Joazeiro, 2009).

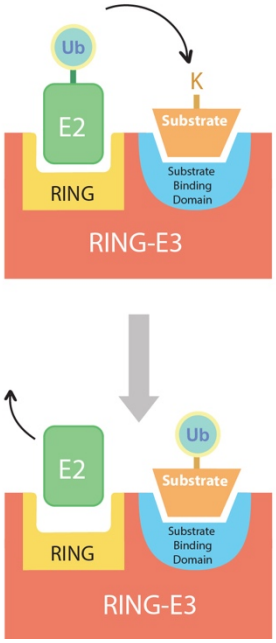

Figure 9. RING-domain E3 Ligase Ubiquitin Transfer

1.6 ZNF598 and RACK1 in RQC

As discussed earlier, among all the RQC factors, ZNF598 mediates the regulatory ubiquitylation of 40S ribosomal proteins, RPS10, RPS20 and RPS3 (Figure 5). RPS10 and RPS20 ubiquitylation is required for inducing stalls upon translating a poly-(A) reporter, as shown in our earlier work: in cell lines with either RPS10 or RPS20 that has mutated ubiquitylation sites, the stall resolution is reduced, resulting in higher readthough of the stall-inducing poly-(A) sequence (Sundaramoorthy et al., 2017).

In addition to ZNF598, Receptor for activated C kinase 1 (RACK1), which is known as Asc1 in yeasts, is a constitutive 40S ribosomal protein to be found next to the mRNA exit tunnel (Figure 5) (Kuroha et al., 2010; Nilsson et al., 2004; Sundaramoorthy et al., 2017). RACK1 recruits activated C kinase, which will phosphorylate eIF6. The phosphorylated eIF6 will dissociate from 60S subunit, allowing the assembly of functional ribosome (Nilsson et al., 2004). Previous studies have shown loss of stall resolution when RACK1 is depleted in 293T cells, and the stall resolution can be rescued by the ribosome-associated RACK1. This finding shows that RACK1 ribosomal association is required for stalling. In addition, RACK1 is required for the DTT (dithiothreitol, a UPR inducer) and HTN (harringtonine, elongation inhibitor)-stimulated RPS2 and RPS3 ubiquitylation (Sundaramoorthy et al., 2017). Clearly, ZNF598 and RACK1 both facilitate ribosomal stalling and are required for overlapping RRub sites. However, in ZNF598 knockout cells, DTT and HTN still induce RPS2 and RPS3 RRub indicating that the RACK1 RRub pathway does not depend on ZNF598 (Sundaramoorthy et al., 2017). Given the fact that RACK1 is a scaffolding protein that participates in various signaling pathways, we

suspect that RACK1 may also interact with ZNF598 and serve as a ribosomal docking site for ZNF598.

My thesis work focuses on understanding how ZNF598 executes poly(A)-induced stall resolution and how this stall resolution is correlated with its RRub activity. The various functional domain found in ZNF598 are yet to be characterized for their stall behavior, 40S ribosome-associated ubiquitylation capability, and their potential roles in forming protein-protein interaction with ribosomal protein RACK1 and self-association with ZNF598.

Chapter 2: Results

2.1 ZNF598 has evolutionally conserved domains

ZNF598 has two types of functional domains: A Really Interesting New Gene (RING) domain (aa 26-69), which is responsible for ZNF598's E3 ligase catalytic activity, and five C2H2-type (X2-Cys-X2,4-Cys-X12-His-X3,4,5-His) Zinc finger domains (Figure 10b), which are commonly known to associate with nucleic acid binding activities and protein interactions (Iuchi, 2001). Four of these C2H2-type Zinc fingers are located in the N-terminus (aa 117-142, aa 187-210, aa 211-239, aa 240-270) and are found to be evolutionally conserved among most vertebrates (Figure 10a). The Zn fingers 2 to 4 (aa 187-210, aa 211-239, aa 240-270) are found as tandem repeats. The last C2H2-type Zinc finger domain lies in the C-terminus (aa 865-866) which is also found to be evolutionally conserved among most vertebrates (Figure 10a). In contrast, Hel2 lacks two C2H2 Zn fingers each in N-terminus and C-terminus (Figure 10 a,b). Lack of this Zn finger in the C terminus in yeast suggests a less significant role for this domain in RQC function. Recent studies have demonstrated that deletion of the last Zinc finger does not impact ZNF598-mediated ribosomal stall resolution (Garzia, Aitor, et al., 2017). In addition, ZNF598 also contains a central unstructured region, which had been observed to harbor RNA binding activity (Garzia, Aitor, et al., 2017) (Figure 10b).

Figure 10. ZNF598 Functional Domain and Truncation Fragment Design
a) phylogenetic tree showing of ZNF598 and its homologs. Predicted RING and ZNF domains are indicated. b) ZNF598 (mammals) vs. Hel2 (yeast) domain comparison
c) c-terminal-truncated ZNF598 fragments T1 to T10.

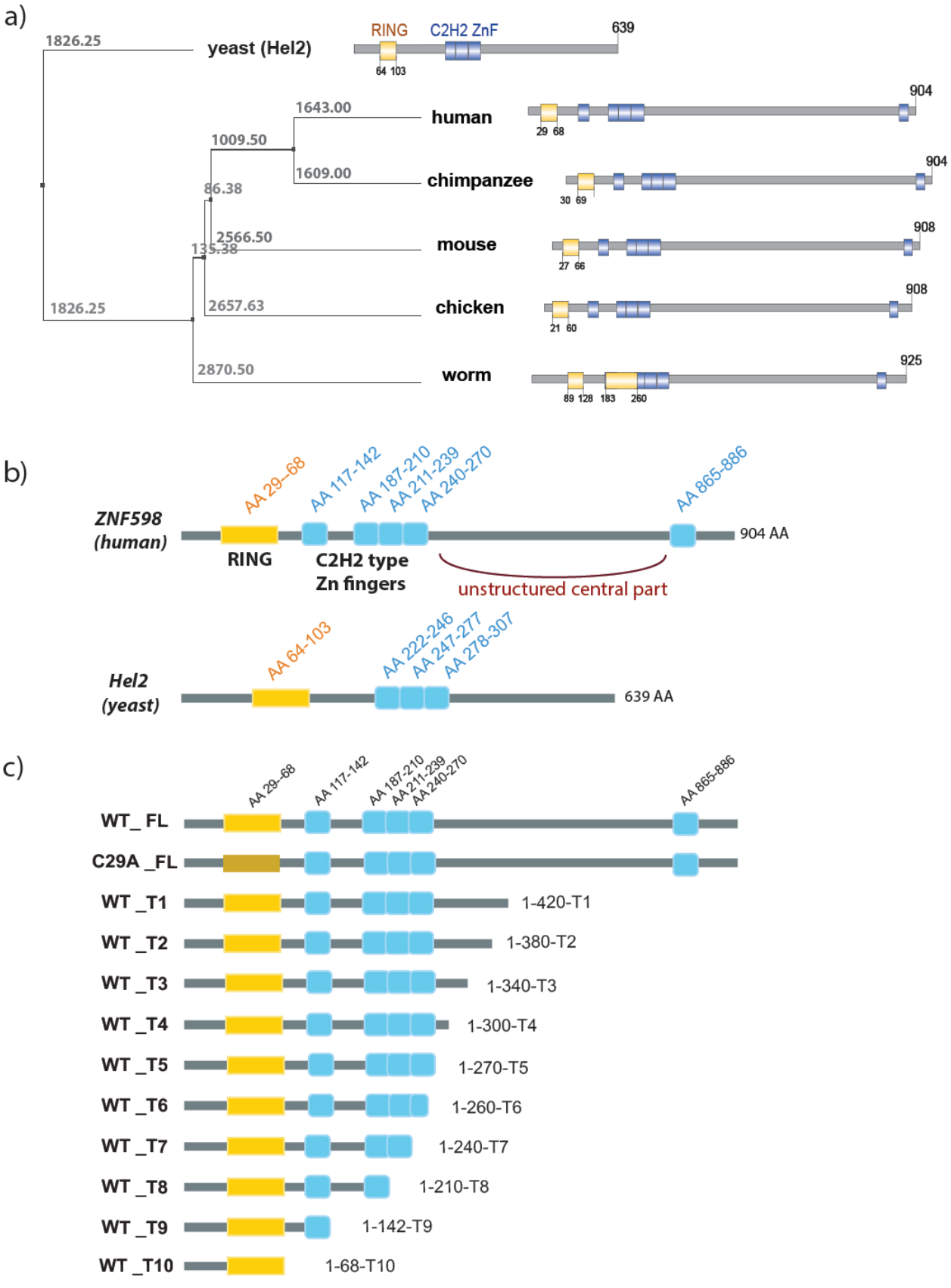
a)
1826.25
yeast (Hel2)
RING
C2H2 ZnF
639
64 103
1643.00
human
904
29 68
1009.50
1609.00
chimpanzee
904
30 69
86.38
2566.50
mouse
908
27 66
2657.63
chicken
908
21 60
1826.25
2870.50
worm
925
89 128 183 260
b)
ZNF598
(human)
AA 29–68
AA 117-142
AA 187-210
AA 211-239
AA 240-270
AA 865-886
904 AA
RING
C2H2 type
Zn fingers
unstructured central part
Hel2
(yeast)
AA 64-103
AA 222-246
AA 247-277
AA 278-307
639 AA
c)
AA 29–68
AA 117-142
AA 187-210
AA 211-239
AA 240-270
AA 865-886
WT_ FL
C29A _FL
WT _T1
1-420-T1
WT _T2
1-380-T2
WT _T3
1-340-T3
WT _T4
1-300-T4
WT _T5
1-270-T5
WT _T6
1-260-T6
WT _T7
1-240-T7
WT _T8
1-210-T8
WT _T9
1-142-T9
WT _T10
1-68-T10

In order to further investigate the role of individual domains of ZNF598 in RQC, we cloned and expressed ZNF598 as distinct protein fragments to isolate the critical region necessary for facilitating 40S-associated RRub. To analyze ribosomal stall events within cells, a FACS-based dual-fluorescence reporter system that was characterized previously in the lab was used (Sundaramoorthy et al 2017). Briefly, the stall reporter consists of a poly cistronic mRNA encoding green fluorescent protein (GFP)-Villin head piece (VHP) Linker-cherry fluorescent protein(ChFP) (Figure 6b, right). Viral 2A peptide skipping sequences bound the linker region allowing equimolar expression of the three proteins. Interestingly, when the linker region is replaced with a poly(A) sequence of 60 bases, a pronounced terminal stall is initiated in the poly(A) region (Figure 6b, left). This ribosome stall event in the poly(A) region skews the equimolar expression of the fluorescent reporters and their ratio is no longer 1:1. We utilized this altered florescence ratio as a direct readout for stall initiation. Our earlier data had shown that in a mammalian cancer cell line, transient overexpressing of the C-terminal truncated constructs of WT ZNF598 resulted in loss of ribosomal stall resolution. Interestingly, the truncated protein behaved as a dominant negative, causing even higher poly(A) read-through than the catalytically inactive ZNF598 (RING domain mutated). This suggests that the ZNF598 C-terminal truncation may inhibit the endogenous ZNF598 function, either by competing with the endogenous protein for ribosomal binding sites or dimerizing with the endogenous ZNF598 and inhibiting E3 ligase function. My proposed research aims to characterize the domains in ZNF598 that are responsible for its ribosomal localization and stall resolution and how the multiple domains in ZNF598 collaborate to execute ribosomal stall resolution.

2.2 Domain specific characterization of ZNF598

ZNF598 truncation constructs were designed based the conserved protein domains it harbors. As mentioned above, the C-terminal Zn finger of ZNF598 is not found in yeast Hel2 despite the fact that Hel2 functions almost identically within the yeast RQC pathway. Therefore, we had designed 10 truncation fragments that excluded the C-terminus (Figure 10c). From truncation 1(all truncation fragments will be mentioned as "T" from now on) to T4, each truncation ends in the unstructured central region, decreasing at lengths of 40 amino acids. T5 to T9 are the fragments truncated at the last amino acid of every Zn finger domain, rendering different number sets of complete Zn fingers. T6 is an exception as it cuts into the fourth Zn finger and is 10 aa shorter than T5. T10 is a RING-only N-terminal fragment. As a negative control, we included a catalytically inactive full-length ZNF598 construct in which a single-nucleotide mutation was introduced in the RING domain (Cys29Ala). We cloned all the fragments into mammalian expression vectors that were lentiviral based for stable expression or regular mammalian vectors for transient expression.

2.3 ZNF598 fragments compete with endogenous ZNF598 and impair RQC function

We performed transient co-transfection of a HEK293T parental cell line with CMV-driven plasmids expressing the ZNF598 truncations and the poly(A) dual-fluorescent reporter plasmid. The ChFP/GFP ratio collected from the FACS analysis was used to monitor the stall resolution. The ChFP/GFP ratio in each fragment transfection was normalized to the ratio observed upon transfection of the poly(A)-stall reporter alone in parental HEK293T as plotted in Figure 11c. The full-length wild type ZNF598 (FL-WT) transfection displayed a strong stall phenotype as its ChFP/GFP ratio was significantly reduced compared to parental with a strong

GFP skewed expression with minimal ChFP expression (Figure 11b). In contrast, the full-length RING-mutant ZNF598 (FL-C29A) transfection exhibited a higher ChFP/GFP ratio compared to parental, suggesting the occurrence of readthrough and impaired stall resolution (Figure 11b, c). Surprisingly, all T1 to T9 transfections produced higher ChFP/GFP ratio than the FL-C29A, suggesting that each truncated version of ZNF598 behaved as a dominant negative and resulted in impaired stall resolution. T1-WT FACS plot is shown as an example of dominant negative in Figure 11b. However, the T10 fragment, RING-only construct, had no dominant negative effect as its ChFP/GFP ratio was on par that observed upon transfection of the stall reporter alone. Overall, the ZNF598 N-terminus plus the beginning of the central region in ZNF598 are unable to induce stalling in response to translation of a poly(A) sequence. Instead, the truncation fragments T1-T9 presented with a dominant negative stall phenotype. The T10 truncation that contains the RING domain alone lacked this dominant negative phenotype.

Figure 11. ZNF598 Fragments Act In a Dominant Negative Manner In the Stall Reporter Assay
a) Immunoblot of the transient-transfected Myc-tagged FL-ZNF598 and Myc-tagged fragments T1-T10.
b) FACS plots of parental HEK293T cells co-transfected with the reporter plasmids and full-length WT ZNF589 (FL-WT), full-length RING-mutant (FL-C29A) and T1 fragment (WT-T1) transfected HEK293. x-axis: ChFP signal level; y-axis: GFP signal level.
c) Fragment and reporter co-transfected HEK293 (fragments shown on right) and corresponding ChFP/GFP ratio relative to parental ratio (left). The first lane marked as "No Frag." represents the only reporter-transfected HEK293T cells.

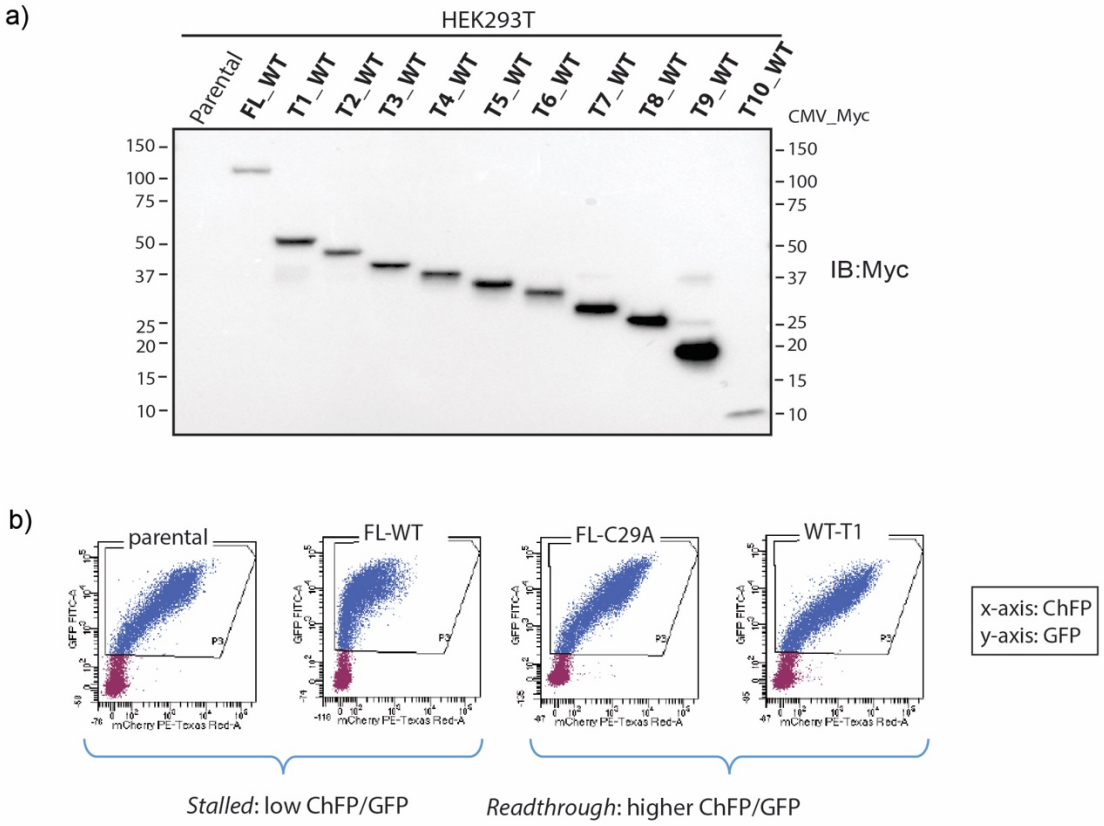
a)
HEK293T
Parental
FL_WT
T1_WT
T2_WT
T3_WT
T4_WT
T5_WT
T6_WT
T7_WT
T8_WT
T9_WT
T10_WT
CMV_Myc
150
100
75
50
37
25
20
15
10
IB:Myc
b)
parental
FL-WT
FL-C29A
WT-T1
x-axis: ChFP
y-axis: GFP
Stalled: low ChFP/GFP
Readthrough: higher ChFP/GFP
c)
Relative ChFP/GFP ratio
Fragments transfected
No_Frag.
WT_ FL
C29A _FL
WT _T1
WT _T2
WT _T3
WT _T4
WT _T5
WT _T6
WT _T7
WT _T8
WT _T9
WT _T10
904
904
420
380
340
300
270
260
240
210
142
68

2.4 The length of ZNF598 dictates RRub site specificity

Our previous studies have shown that RPS10 and RPS20 RRub are required for a robust poly(A)-induced stall phenotype (Sundaramoorthy et al., 2017). In order to investigate whether the stall readthrough is actually caused by the loss of RPS10 and RPS20 RRub, we established stable expression of ZNF598 and its fragments in HEK293, HCT116 and HCT116 ZNF598 knock out cells (Sundaramoorthy et al 2017). We validated the expression of the fragments (Figure 12a, top panels) and blotted for ubiquitin-modified RPS10 and RPS20. In HEK293T and HCT116 overexpression cell lines, we found that fragments T1 to T7 induced RPS10 ubiquitylation (Figure 12a, b). The ubiquitin-modified RPS10 protein is shown as the lower band (~25kD) of the doublet bands in the anti-RPS10 long exposure blot. Truncation fragments that are shorter than T7, such as T8, T9 and T10, were not able to induce RPS10 RRub as their ubiquitin-modified bands are not significantly more intense than that in control cells (Figure 12a, b). In both HEK293T and HCT116 stable cells, RPS20 ubiquitylation was only observed in the longer fragments, T1 to T4, with the sequences spanning beyond the fourth Zn finger (Figure 12a, b). The T4 fragment displayed the strongest induction of RPS20 RRub the most among all these longer fragments, which is noticeable in the HCT116 RPS20 blot (Figure 12b).

Figure 12. Length of C Terminal Truncations of ZNF598 Dictates RRub Site Specificity
HA-tagged T1 to T10 ZNF598 fragments were stably expressed in 293T (a) or HCT116 (b) cells. Whole cell extracts from each cell line were prepared and immunoblotted as indicated.

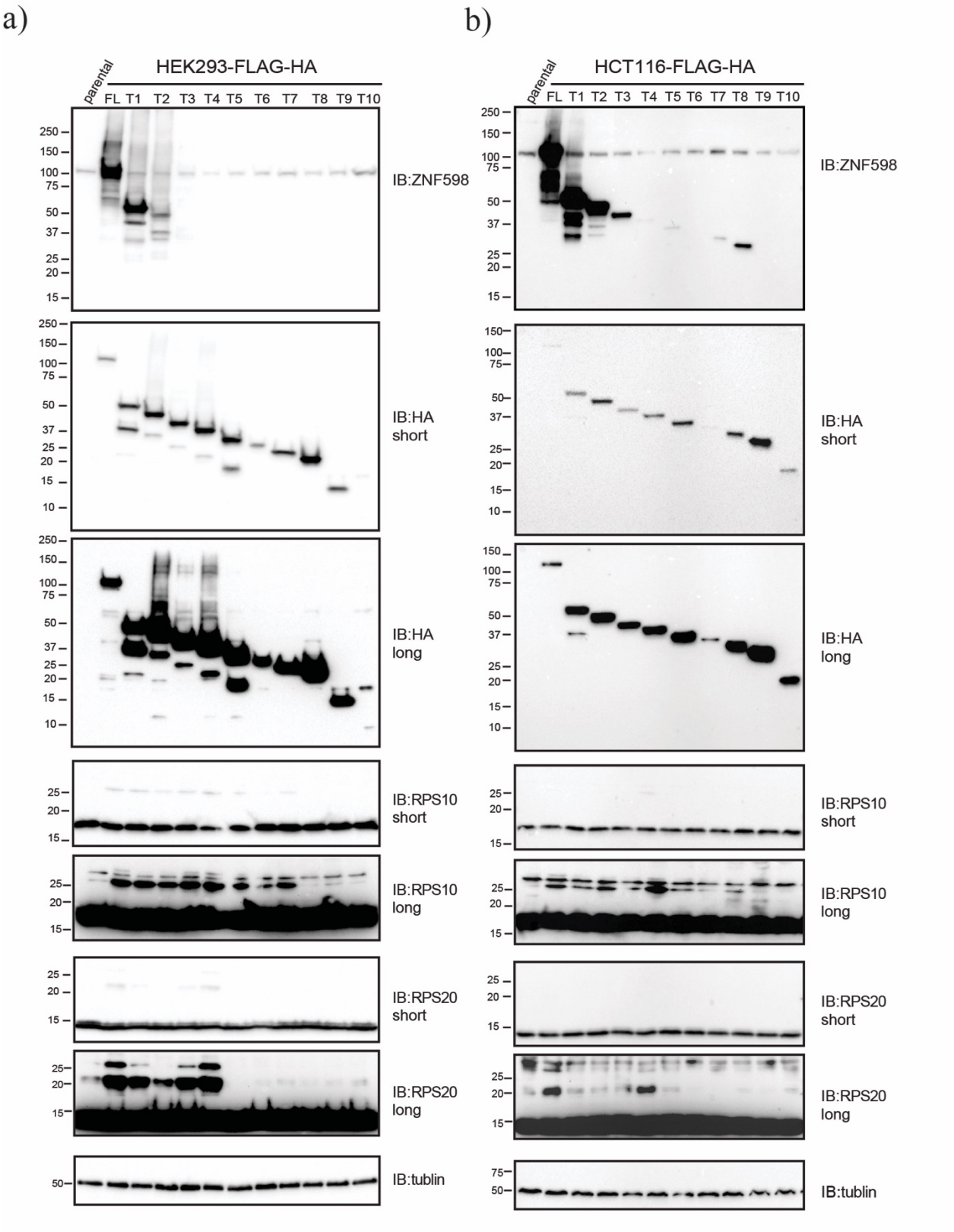
a)
HEK293-FLAG-HA
parental
FL T1 T2 T3 T4 T5 T6 T7 T8 T9 T10
IB:ZNF598
IB:HA short
IB:HA long
IB:RPS10 short
IB:RPS10 long
IB:RPS20 short
IB:RPS20 long
IB:tublin
b)
HCT116-FLAG-HA
parental
FL T1 T2 T3 T4 T5 T6 T7 T8 T9 T10
IB:ZNF598
IB:HA short
IB:HA long
IB:RPS10 short
IB:RPS10 long
IB:RPS20 short
IB:RPS20 long
IB:tublin

2.5 RACK1 regulates ZNF598 C terminal truncations RRub activity

Our earlier studies had shown that the transient knock down of RACK1 in HEK293T parental significantly increased the readthrough ChFP/GFP ratio but exhibited no effect in stall-impaired ZNF598 knockout HEK293T cells (Sundaramoorthy et al., 2017). In the light of that, we suspect that ZNF598 may act through ribosome-residing RACK1 protein for its RRub activity. Therefore, we decided to perform the transient knock down of RACK1 in T5 overexpression HCT116 cell line. The RACK1 knockdown treatment (Figure 13, right column) decreased the RPS10 ubiquitylation compared to siRNA control. This RPS10 RRub down-regulation by siRACK1 knockdown is similar to the pattern observed in FL-WT overexpression (Figure 7, middle column). In addition, the complete lack of RPS20 RRub bands is consistent with our RRub immunoblots (Figure 12), that T5 has RPS10-specific activity.

Figure 13. RACK1 Knock Down Reduces RPS10 Ubiquitylation in the T5 Overexpression Cell Line
HCT116 parental, HA-FLAG(NTAP)-tagged FL-WT and HA-FLAG(NTAP)-tagged T5 fragment overexpression stable cells were transfected with control siRNA or three separate siRNA oligos targeting RACK1. Cell lysates were analyzed by SDS-PAGE and immunoblotted with indicated antibodies.

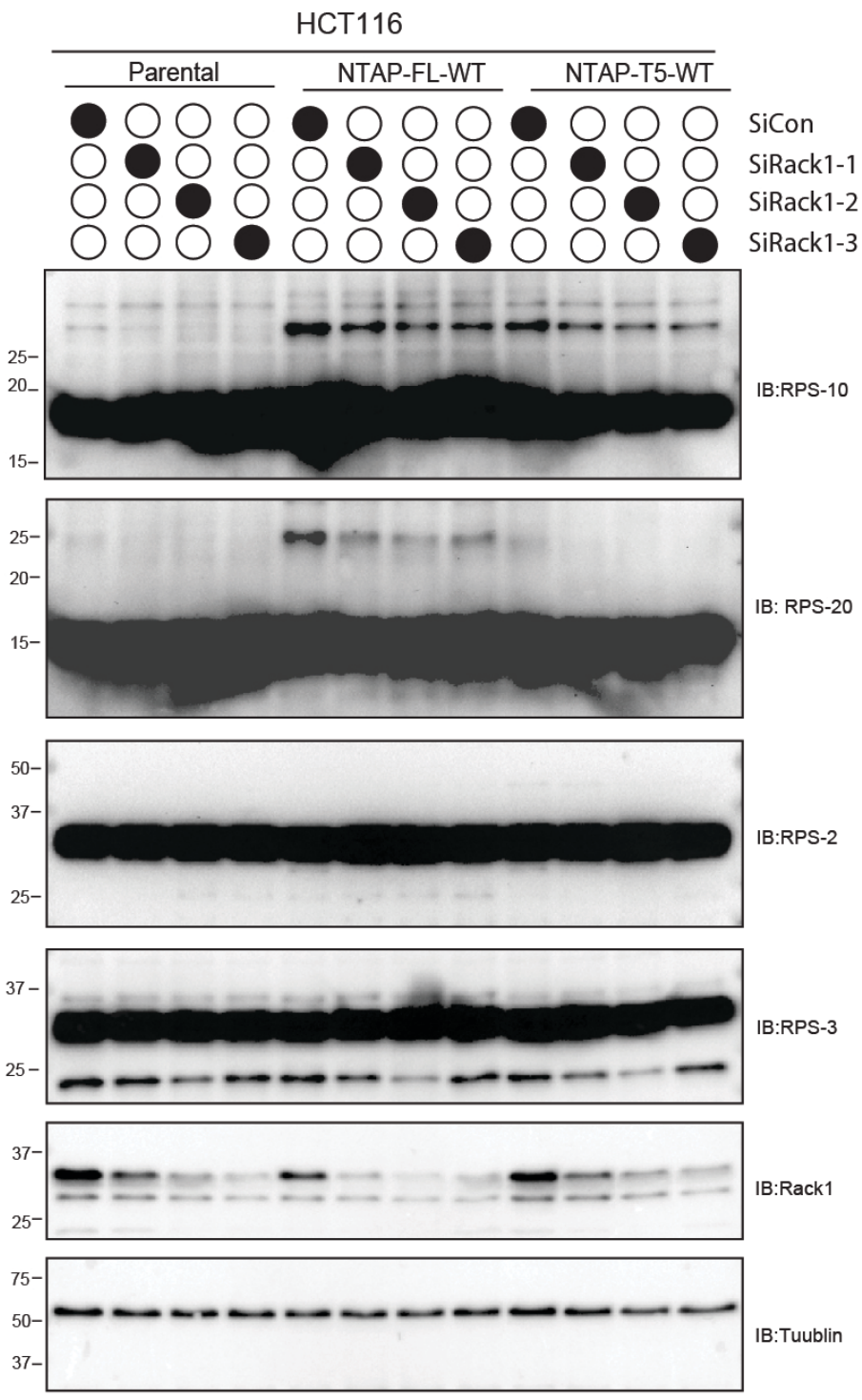
HCT116
Parental
NTAP-FL-WT
NTAP-T5-WT
SiCon
SiRack1-1
SiRack1-2
SiRack1-3
25–
20–
15–
IB:RPS-10
25–
20–
15–
IB: RPS-20
50–
37–
25–
IB:RPS-2
37–
25–
IB:RPS-3
37–
25–
IB:Rack1
75–
50–
37–
IB:Tuublin

2.6 Fragments T5 and T9 Immunoprecipitated with FL-WT ZNF598

To further explore how the dominant negative fragments may impact the endogenous or WT ZNF598 function, we performed immunoprecipitation to examine a possible protein-protein interaction between the ZNF598 fragments and FL-WT ZNF598. We selected T5 (RPS10-specific RRub), T9 (smallest dominant negative fragment), T10 (RING-only fragment that did not increase readthrough) to be transiently transfected into FLAG-tagged ZNF598 overexpressing HEK293T. Immunoblots for Myc-tagged fragments on the FLAG-FL-WT pull-down proteins (Figure 14, lower right) shows the presence of T5 and T9. However, T10 is not seen in the same blot nor in the anti-Myc blot (Figure 14, center and lower in the middle column), indicating T10 may be not well expressed or have low transfection efficiency. Overall, our IP assay provides the evidence that T5 and T9, the two dominant negative fragments, interact with FL-WT ZNF598.

Figure 14. Fragments T5 and T9 Interact with WT ZNF598
Myc-tagged FL-WT, T5, T9, and T10 were transfected into cells with stable expression of Flag-HA-tagged full-length wild type ZNF598 Input lysates (left) of the transfected cells were analyzed by SDS-PAGE and immunoblotted with the antibodies as indicated. Lysates were also immunoprecipitaed using anti-Myc agarose beads (middle) or anti-FLAG agarose beads (right) followed by SDS-PAGE and immunoblotting with antibodies indicated.

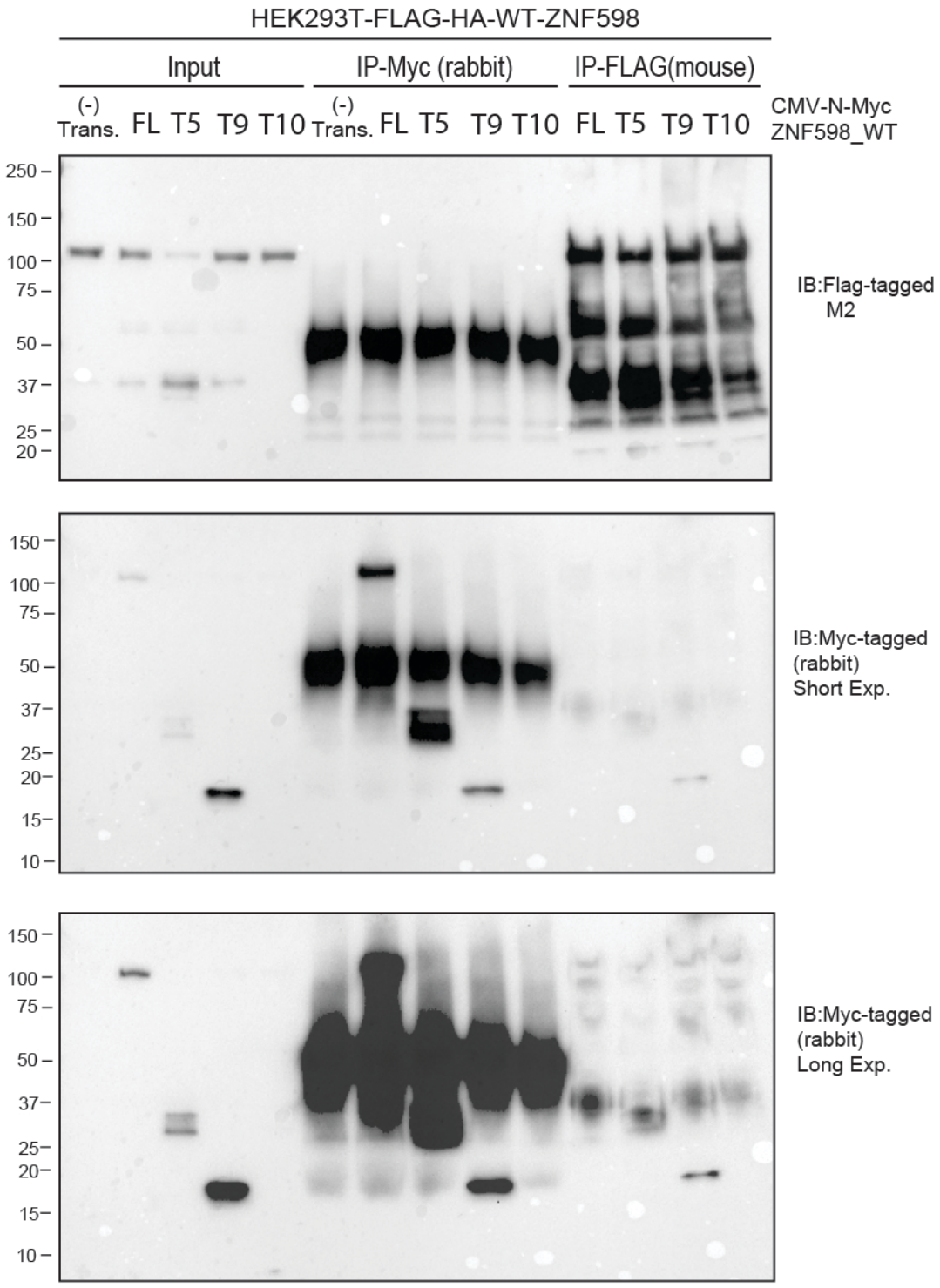
HEK293T-FLAG-HA-WT-ZNF598
Input
IP-Myc (rabbit)
IP-FLAG(mouse)
(-) Trans.
FL
T5
T9
T10
(-) Trans.
FL
T5
T9
T10
FL
T5
T9
T10
CMV-N-Myc ZNF598_WT
250
150
100
75
50
37
25
20
IB:Flag-tagged M2
150
100
75
50
37
25
20
15
10
IB:Myc-tagged (rabbit) Short Exp.
150
100
75
50
37
25
20
15
10
IB:Myc-tagged (rabbit) Long Exp.

Chapter 3: Discussion

3.1 ZNF598 N-terminal Length Determines RRub Specificity

The smallest fragment that can induce RPS10 RRub is T7 which suggests that the first three zinc fingers (two in the tandem repeat) are the minimal N-terminal truncation within ZNF598 that can support RPS10 RRub (Figure 12). T4 and all the longer fragments (T3, T2 &T1) induce both RPS10 and RPS20 RRub, behaving identically with FL-WT ZNF598 in terms of their RRub activity. The observation that the T5 fragment (contains the first 4 Zn fingers) is unable to induce RPS20, but T4 (first 4 Zn fingers plus a stretch of 30 a.a in the central region) can suggests a significant role of the central unstructured region in facilitating RPS20 ubiquitylation. These results indicate that ZNF598's ribosomal substrate specificity is intrinsically linked to its functional domains and is length-dependent.

3.2 RPS10 and RPS20 RRub is required but not sufficient for ribosome stall resolution

The observation that the T4 to T1 ZNF598 fragments facilitate RPS10 and RPS20 RRub in a manner that is identical to full-length ZNF598, but are not able to enhance ribosome stall resolution in the poly(A)-induced stall reporter assay suggest that that RPS10 and RPS20 ubiquitylation are required but not sufficient to for faithful resolution of ribosome stalls. Speculatively, the stall phenotype might be a trio of features that endogenous full-length ZNF598 harbors, i.e; RPS10 and 20 ubiquitylation along with RNA binding activity. In what capacity the central unstructured region adds to the stall phenotype will be taken up for further characterization.

3.3 Rescue of stalled ribosomes requires the central unstructured domain of ZNF598

Garzia and colleagues demonstrated that the defect in ribosome stall resolution observed in ZNF598 knock out cells could be rescued by a truncated version of ZNF598 (Garzia et al., 2017). Their results showed that ZNF598 fragments with the last Zn finger and the C-terminus deleted (a.a.1-864, 1-749) were able restore the stall resolution with a repressed readthrough level similar to that of full-length ZNF598. However, the central-deleted fragment (a.a. 1-290) which is 10 a.a. shorter than our T4 construct, displayed an increased readthrough level but not as high as that in the RING-deleted fragment rescue, suggesting a partially impaired stall surveillance. The same research group also conducted a PAR-CLIP experiment to investigate the RNA-binding activity of the truncated fragments and discovered that central-deleted fragment no longer binds to RNA (Garzia et al., 2017). Combined with our data showing the T1-T4 fragments can mediate RRub but cannot rescue the defect in ribosome stall resolution suggests that the ZNF598 central unstructured part that harbors an RNA-binding activity is critical for stall resolution.

3.4 RACK1 is required for ZNF598-dependent RPS10 and RPS20 ubiquitylation.

Both FL-WT ZNF598 and the T5 fragment overexpression in HCT116 cells resulted in decreased RPS10 ubiquitylation in siRACK1 treatment comparing to control (Figure 13). FL-WT overexpression cells also displayed decreased RPS20 ubiquitylation upon RACK1 knock down. These observations suggest a possible interaction between RACK1 and ZNF598, and this interaction is likely to be involved in ZNF598's RRub regulation. It is consistent with our previous finding that RACK1 and ZNF598 both facilitate ribosomal stall resolution and are likely to be involved in the same RQC pathway (Sundaramoorthy et al., 2017). Knock down of

ZNF598 shows an elevated readthough level, but with the additional RACK1 knock down does not further increase the readthrough, implicating that RACK1 is likely to function upstream of ZNF598 in poly(A)-associated RQC (Sundaramoorthy et al., 2017). My SiRNA knock down experiment with the T5 fragments combined with the evidence provided in our previous publication supports our hypothesis that ZNF598 binds to RACK1 as a docking site for its ribosomal localization.

RACK1 is found to be located in the head region of 40S ribosomal subunit, adjacent to the mRNA exit tunnel. Structural analysis shows that RACK1 directly interacts with ribosomal RNA (Nilsson et al., 2004). Moreover, RACK1's recruitment of PKC, from a structural perspective, suggests the binding of a RNA-associated protein (Nilsson et al., 2004).

We suspect that ZNF598 ribosomal localization might require RACK, through the rRNA binding activity of RACK1. The central region of ZNF598 that harbors the RNA-binding activity, as shown by Garzia and colleagues, may be essential for stall resolution by seizing the mRNA at its exit tunnel thus preventing the ribosome reading further into the 3' end.

3.5 ZNF598 N-terminal fragments interfere with endogenous ZNF598's ribosomal activity leading to a dominant negative stall phenotype

The observation that the RING-mutant ZNF598 transfection results in increased readthough in the poly(A) stall reporter assay can be explained by a simple competition model in which the inactive exogenous ZNF598 competes with endogenous ZNF598 for ribosomal binding but is unable to recruit E2 enzymes to induce RRub. In cases of the fragment

transfection, the readthrough is even higher than the RING-mutant, implicating the fragments might interfere with endogenous ZNF598 in a different way. One possible explanation is that the fragments might have higher affinity to ribosomes than FL ZNF598 due to the smaller sizes thus undergoing less steric hindrance or being structurally more open for binding. In addition, we also postulate that the fragments will form dimers or oligomers with endogenous ZNF598 and their interactions may trigger autoubiquitylation of both endogenous ZNF598 and the expressed fragments leading to the degradation of both components (Figure 15b). In support of this hypothesis, in HEK293T cell lines that stably overexpress the ZNF598 fragments, the endogenous ZNF598 expression levels are reduced, T4 showing the highest reduction (Figure 12). A time-course protein stability pulse-chase assay with translational inhibitor cycloheximide would be required to tease out this phenotype.

In several scenarios RING ligases dimerize either as homomeric or heteromeric interactors to ubiquitylate their substrates and dimerization enhances their E3 ligase activity MDM2-MDx, Brca1-Bard1 exemplify heterodimeric RING ligases while RNF4, Traf, Siah,and cIAP homodimerize ((Deshaies and Joazeiro, 2009; Liew et al., 2010). We suspect that ZNF598 may also form dimers at its native state, either through its RING domain or the Zinc fingers or both. We propose a model in which the binding of the dimerized ZNF598 to the ribosome is able to stabilize ubiquitin transfer from E2, resulting in ubiquitylation of both RPS10 and RPS20, each by an individual ZNF598 in the dimer. However, the fragments of ZNF598 may pose several more complex scenarios:

1) Fragments (T7-T5) that can localize to the ribosomes alone but are unable to recruit another ZNF598 due to the lack of a proper binding sequence, resulting in partial RRub that is only on RPS10 (Figure 15a).

2) Fragments that can bind to ribosome in a dimer form or can bind to the ribosome then recruit another ZNF598 to induce ubiquitylation on both RPS10 and RPS20 sites, such as T1 to T4. The stall resolution is still lost because the central RNA-binding region is missing (Figure 15a).

Autoubiquitylation mediated by the fragments as seen in the (Figure 12) suggests a cross-stabilization phenotype for the fragments. The fragments preferentially binding to the ribosomes might allow its stabilization whereas the non-ribosome localized versions might undergo autoubiquitylation mediated degradation by the ubiquitin proteasome system (UPS) (Figure 15b). The IP experiments does hint that T5 and T9 capable of interacting with the full-length protein can mediate dimerization induced autoubiquitylation and degradation (Figure 14).

Figure 15. A Proposed Model for ZNF598 N-terminal Truncation RRub Activities and Stall Behavior
a) A speculative model of the dimerized endogenous ZNF598 and ZNF598 N-terminal truncations along with their RRub activities and stall phenotypes.
b) A speculative model of dimer-induced autoubiquitylation of Wt-ZNF598 and ZNF598 N-terminal truncations that potentially lead to the dominant negative stall phenotypes.

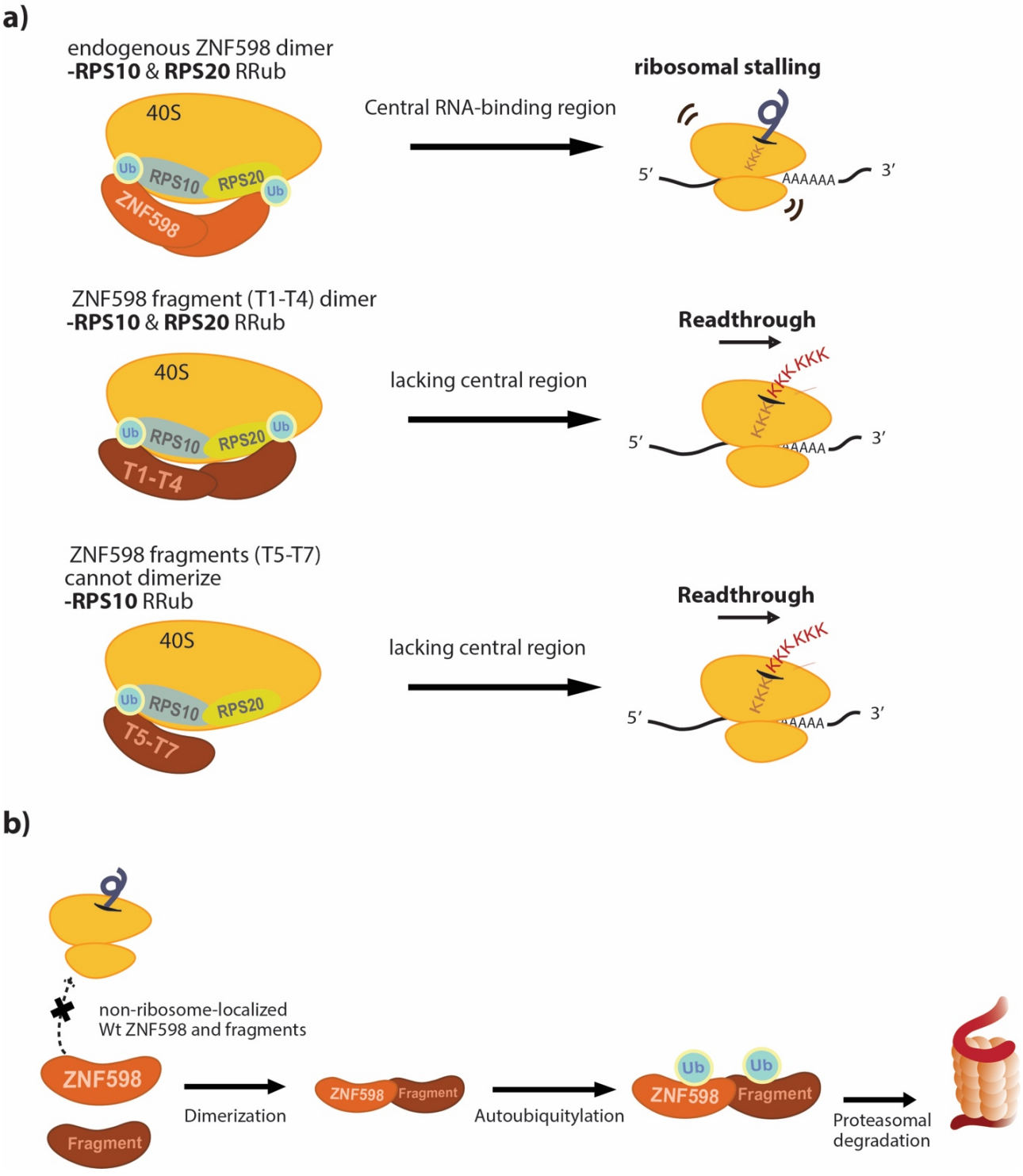
a)
endogenous ZNF598 dimer
-RPS10 & RPS20 RRub
40S
Ub
RPS10
RPS20
Ub
ZNF598
Central RNA-binding region
ribosomal stalling
KKK
5′
AAAAAA
3′
ZNF598 fragment (T1-T4) dimer
-RPS10 & RPS20 RRub
40S
Ub
RPS10
RPS20
Ub
T1-T4
lacking central region
Readthrough
KKK-KKK
KKK
5′
AAAAA
3′
ZNF598 fragments (T5-T7)
cannot dimerize
-RPS10 RRub
40S
Ub
RPS10
RPS20
T5-T7
lacking central region
Readthrough
KKK-KKK
KKK
5′
AAAAA
3′
b)
non-ribosome-localized
Wt ZNF598 and fragments
ZNF598
Fragment
Dimerization
ZNF598
Fragment
Autoubiquitylation
Ub
Ub
ZNF598
Fragment
Proteasomal
degradation

In the case of T10 (only-RING), it may have lost the Zn fingers that stabilize the dimer interaction and ribosomal localization, leaving the endogenous ZNF598 unperturbed, neither competing or degrading the endogenous ZNF598. It provides a potential explanation for why the poly(A)-induced stall resolution in T10 transfected cells is similar to the control experiments in which no ZNF598 is introduced.

Overall, my work extends the role of ZNF598 in ribosome ubiquitylation and has identified critical requirements for the following site-specific activities (Figure 16):

1) RPS10-ubiquitylation requires N-terminal RING and at least the first three Zinc fingers domains
2) RPS10 and RPS20 ubiquitylation requires N-terminal RING, all four Zinc fingers and at least the beginning 30 a.a sequence in central region of ZNF598.

In addition, we also conclude that ZNF598's central region harbors a stall-inducing ability in poly(A)-triggered ribosomal stall, possibly with its RNA-associated activity.

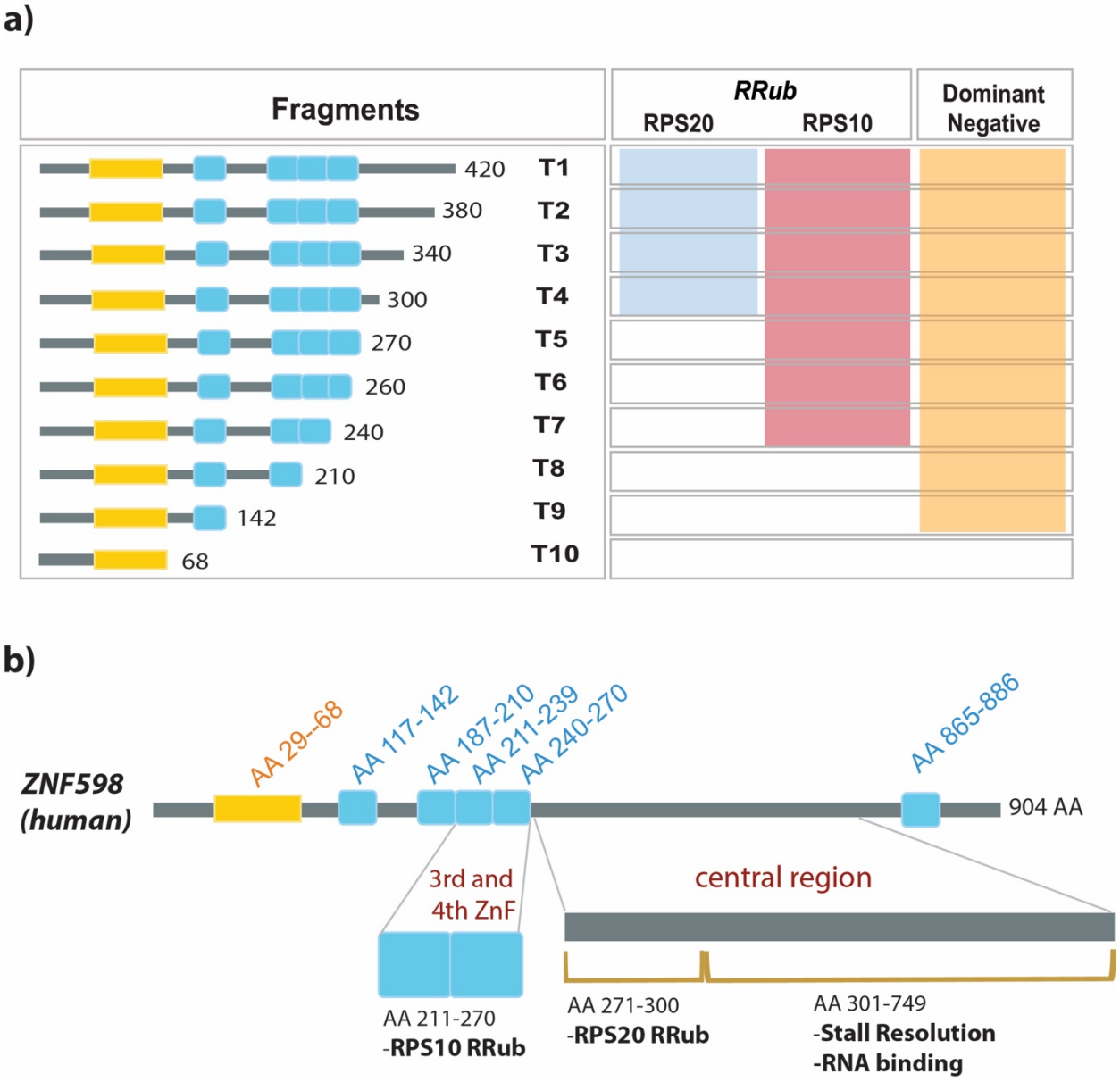

Figure 16. Characterizing the RQC Properties of the Conserved Functional Domains of ZNF598
a) Fragment constructs are listed along with their RRub specificity and stall behaviors.
b) Characterization of ZNF598 functional domains in summary.

Material and Methods

Vector Cloning

The Gateway Cloning system (Invitrogen) was used to clone all fragment constructs into pDEST-CMV-Myc (for FACS) and pDEST-pHAGE-FLAG (for stable expression cell lines) destination vectors for transfection in mammalian cell lines. The fragment PCR products were flanked with attB recombination sites in order to enter the Gateway cloning system. The PCR primer sequences with attB sites incorporated are shown as below:

Primer			Primer sequences (5' to 3')
Forward		all fragments	GGGGACAACTTTGTACAAAAAAGT TGGCatggcggcggcgggggc
Reverse	T1 (1_420)	BP_ZNF598_1_420_ stop_Rev	GGGGACAACTTTGTACAAGAAAGT TGGctagcctgtcaccgagaaggcttcttg
	T2 (1_380)	BP_ZNF598_1_380_ stop_Rev	GGGGACAACTTTGTACAAGAAAGT TGGctacgccgctgcctcctccttc
	T3 (1_340)	BP_ZNF598_1_340_ stop_Rev	GGGACAACTTTGTACAAGAAAGTT GGctattcttccctttgtacctccagcttcctc
	T4 (1_300)	BP_ZNF598_1_300_ stop_Rev	GGGGACAACTTTGTACAAGAAAGT TGGctagacccccctcgttccggcgc
	T5 (1_270)	BP_ZNF598_1_270_ stop_Rev	GGGGACAACTTTGTACAAGAAAGT TGGctagtggcaggccgtcctgtgggc
	T6 (1_260)	BP_ZNF598_1_260_ stop_Rev	GGGGACAACTTTGTACAAGAAAGT TGGctagatctcggtgcggaaggcgtg
	T7 (1_240)	BP_ZNF598_1_240_ stop_Rev	GGGGACAACTTTGTACAAGAAAGT TGGctaaaagtgcttctcccggaagtgctcacgc
	T8 (1_210)	BP_ZNF598_1_210_ ifx_Rev	GGGGACAACTTTGTACAAGAAAGT TGGctagtggtcgcggcgcaggtgc
	T9 (1_187)	BP_ZNF598_1_142) _stop_Rev	GGGGACAACTTTGTACAAGAAAGT TGGctaatgctgcctccgcatgtgctgc
	T10 (1_68)	BP_ZNF598_1_68_if x_Rev	GGGGACAACTTTGTACAAGAAAGT TGGctagcacacggcgcagtagcgctgc

Stable Cell Lines Generation

The destination plasmids containing FLAG-HA-tagged fragments were lentiviral transduced into HEK293T, HCT116 and ZNF598 K.O. HCT116 cells. Using TransIT 293

transfection reagent with the helper plasmids pHAGE - GAG-POL; pHAGE – VSVG; pHAGE – tat1b; pHAGE – rev. and pHAGE-ZNF fragments, in HEK293T cells for producing lentivirus . The virus-containing media was filtered and added with 2 ul of 6mg/ml polybrene per 1.5ml of media, and the mixture was added to the target cell lines seeded at ~30% confluency. Around 2-3 days of recovery, the cells entered 2 mg/ml Puromycin selection.

The ZNF598 knockout HCT116 cell line was generated previously using CRISPR/Cas9 genome editing. The ZNF598 knockout cell line refers to clone N in our previous study(Sundaramoorthy et al., 2017).

Dual Fluorescence Stall Reporter Plasmids

The dual-fluorescence reporter plasmid was a generous gift from Manu Hegde and Susan Shao (MRC, Cambridge, UK).

FACS Stall Assay

The dual fluorescence reporter plasmids transfected into HEK293T cells using Lipofectamine 2000 (Thermo Fisher) according to manufacturer guidelines. Each fragment was transfected in triplicate. Cells were harvested 48 hours post-transfection. The resulting GFP and ChFP fluorescence intensity was measured on a LSRFortessa X-20 cytometer (BD Biosciences), followed by FACS analysis with FlowJo (version 9.1).

Immunoblotting

The cells were harvested and reesuspended in lysis buffer (8 M urea, 50 mM Tris-Cl, pH 8.0, 75 mM NaCl, 1 mM NaF, 1 mM NaV, 1 mM b-glycerophosphate, 40 mM NEM) with EDTA-free Protease Inhibitor Cocktail (Roche Diagnostics, 5056489001). Cells were kept on ice

throughout preparation. After the lysis buffer was added, and cells were sonicated briefly (10 s at output of 3 W on a membrane dismembrator model 100 (Fisher Scientific) with a microtip probe and centrifuged for 10 min at 21,000 x *g* at 4 °C. The supernatants were transferred to new tubes, and were kept on ice the whole time. The lysate protein concentrations were measured by BCA Protein Assay (Thermo Scientific Pierce, 23225). Laemmli sample buffer with β-mercaptoethanol was then added to cell lysates. Cell lysates were heated at 95 °C for 5 min, and centrifuged for 5 seconds. The prepared lysate samples were resolved on Tris-glycine SDS-polyacrylamide gel electrophoresis (SDS -PAGE) gel (Bio-Rad 4%-20% gradient gel for anti-HA blot; 12% or 15% gels for anti-RPS10 and anti-RPS20 blots). Proteins were transferred using Bjerrum semi-dry transfer buffer (48 mM Tris Base, 39 mM Glycine-free acid, 0.0375% SDS, 20% MeOH, pH 9.2) to PVDF membranes (Bio-Rad Immun-Blot, 1620177) using a semi-dry transfer apparatus (Bio-Rad Turbo Transfer) for 30 min at 25V. Immunoblots were developed using Clarity Western ECL Substrate (Bio-Rad, 1705061), and imaged on a Bio-Rad Chemi-Doc XRS+ system. Blots images were processed using Imagelab (Biorad) software and were finished in Adobe Illustrator for preparing final images.

RACK1 Knock Down

siRNA oligos targeting the RACK1 mRNA were reverse transfected using RNAiMAX (Invitrogen) by following manufacturer guidelines. Three RACK1 knockdown oligos were used for each knock-down treatment to form RNAi duplex-Lipofectamine RNAiMAX complex. The SiRACK1 oligo sequences is list below:

siRNA Targeting Gene	Duplex Catalog Number	Oligo Sequences
RACK1	D-006876-02	GAUAAGACCAUCAUCAUGU
	D-006876-03	CCAAGGAUGUGCUGAGUGU
	D-006876-04	GAGAUAAGACCAUCAUCAU

The fragment overexpressing HCT116 cells were harvested and incubated with the RNAiMAX transfection reagent for 20 minutes. The cells were seeded in 6-well plates at density which will give 30~50% confluency after 24 hours. Cells were split 1:3 on the following day. 72 hours post-transfection, cells were harvested and pellet for western blotting. DMEM without pen/strep was used during the whole siRNA experiment.

Immunoprecipitation

FL-WT-overexpressing HCT116 cells were transfected with Myc-tagged fragment plasmids on 10cm plates using Lipofectamine 2000 (Thermo Fisher) according to manufacturer guidelines.

Cells are harvest 48 hours post-transfection followed by lysis using MCLB (50 mM Tris-Cl, pH 7.8, 150 mM NaCl, 0.5% NP40, 1 mM NaF, 1 mM NaV, 1 mM b-glycerophosphate, 5 mM NEM) with EDTA-free Protease Inhibitor Cocktail (Roche Diagnostics, 5056489001). The lysis sample were incubated on ice for 5 minutes and sonificated for 3 seconds (short sonification to lyse open the cells without disrupting protein interaction) at output of 3 W on a membrane dismembrator model 100 (Fisher Scientific), immediately followed by another on-ice incubation for 5 minutes to cool down the samples. Cells were centrifuged for 10 min at 21,000 x *g* at 4 C. The supernatants were transferred to new tubes as the lysate, and concentrations were measured by BCA Protein Assay (Thermo Scientific Pierce, 23225). 30~50 ul of lysate was saved and

added with Laemmli sample buffer with b-mercaptoethanol as the Input to be frozen down for Western Blot analysis later. 15ul of the 50% slurry volume of anti-Myc or anti-FLAG resin beads per IP sample were equilibrated 4 times, each wash with equivalent volume of MCLB+PIs lysis buffer. Prepare lysate containing 500ug of total proteins and make up to the total volume of 300ul with MCLB+PIs lysis buffer. 15ul of equilibrated 50% resin slurry was added to the lysate followed by 1-hr incubation at 4 °C with rotation. After biniding, the samples were spun down (3000rpm for 1 minute) and washed with Wash buffer(50 mM Tris-Cl, pH 7.8, 150 mM NaCl, 0.5% NP40) 4 times with the same centrifugation setting between each. P311 tips were used to remove all the liquid from the beads after the last wash. To prepare the IP pull-down samples, Laemmli sample buffer with b-mercaptoethanol was added to the beads which stripped the protein bound to the beads. Inputs and IP pull-down samples were analyzed by immunoblotting using antibodies from a different species than that of resin-bound antibodies.

Antibodies

Antibodies	Manufacturer	Catalog No./Clone number/Product number
RPS2 (rabbit polyclonal)	BETHYL LABORATORIES INC	A303-794A
RPS3 (rabbit polyclonal)	BETHYL LABORATORIES INC	A303-840A
RPS10 (rabbit monoclonal)	Abcam	EPR8545
RPS20 (rabbit monoclonal)	Abcam	EPR8716
HA (rabbit polyclonal)	SIGMA	H6908
ZNF598 (rabbit polyclonal)	SIGMA	HPA041760
c-Myc (mouse monoclonal)	SANTA CRUZ BIOTECHNILOGY INC	9E10
Myc-tag (rabbit monoclonal)	CellSignal	71D10
FLAG M2(mouse monoclonal)	SIGMA	F3165
FLAG(rabbit polyclonal)	SIGMA	F7425
Rabbit IgG(H+L) HRP conjugate	W4022	Promega
Mouse IgG(H+L) HRP conjugate	W4021	Promega

IP Agarose Resin

Conjugated Antibodies	Manufacturer	Catalog No./Clone number/Product number
c-Myc-conjugated (rabbit)	SIGMA	A7470
FLAG M2	SIGMA	A2220

This whole thesis will be prepared for submission for publication of the material. Li, Ruoyu; Sundaramoorthy, Elayanambi. The thesis authors are the primary investigators and the authors of the materials.

References

Arthur, L.L. Mechanism of Gene Regulation by Coding PolyA Tracks. 222.

Ascano, M., Jr., N. Mukherjee, et al. (2012). "FMRP targets distinct mRNA sequence elements to regulate protein expression." Nature 492(7429): 382-386.

Bengtson, M.H., and Joazeiro, C.A.P. (2010). Role of a ribosome-associated E3 ubiquitin ligase in protein quality control. Nature *467*, 470–473.

Borden, K.L., and Freemont, P.S. (1996). The RING finger domain: a recent example of a sequence—structure family. Current Opinion in Structural Biology 6, 395–401.

Brandman, O., and Hegde, R.S. (2016). Ribosome-associated protein quality control. Nat Struct Mol Biol 23, 7–15.

Brandman, O., J. Stewart-Ornstein, et al.(2012). "A ribosome-bound quality control complex triggers degradation of nascent peptides and signals translation stress." Cell 151(5): 1042-1054.

Brandman, O., Stewart-Ornstein, J., Wong, D., Larson, A., Williams, C.C., Li, G.-W., Zhou, S., King, D., Shen, P.S., Weibezahn, J., et al. (2012). A Ribosome-Bound Quality Control Complex Triggers Degradation of Nascent Peptides and Signals Translation Stress. Cell *151*, 1042–1054.

Brule, C. E. and E. J. Grayhack (2017). "Synonymous Codons: Choose Wisely for Expression." Trends Genet 33(4): 283-297.

Celik, A., Kervestin, S., and Jacobson, A. (2015). NMD: At the crossroads between translation termination and ribosome recycling. Biochimie *114*, 2–9.

Coller, J., and Parker, and R. (2004). Eukaryotic mRNA Decapping. Annual Review of Biochemistry *73*, 861–890.

Defenouillere, Q., Y. Yao, et al. (2013). "Cdc48-associated complex bound to 60S particles is required for the clearance of aberrant translation products." Proc Natl Acad Sci U S A 110(13): 5046-5051.

Defenouillère, Q., Zhang, E., Namane, A., Mouaikel, J., Jacquier, A., and Fromont-Racine, M. (2016). Rqc1 and Ltn1 Prevent C-terminal Alanine-Threonine Tail (CAT-tail)-induced Protein Aggregation by Efficient Recruitment of Cdc48 on Stalled 60S Subunits. Journal of Biological Chemistry *291*, 12245–12253.

Deshaies, R.J., and Joazeiro, C.A.P. (2009). RING Domain E3 Ubiquitin Ligases. Annual Review of Biochemistry *78*, 399–434.

Dever, T.E., and Green, R. (2012). The Elongation, Termination, and Recycling Phases of Translation in Eukaryotes. Cold Spring Harb Perspect Biol *4*.

Dimitrova, L.N., Kuroha, K., Tatematsu, T., and Inada, T. (2009). Nascent peptide-dependent translation arrest leads to Not4p-mediated protein degradation by the proteasome. J. Biol. Chem. *284*, 10343–10352.

Doma, M. K. and R. Parker (2006). "Endonucleolytic cleavage of eukaryotic mRNAs with stalls in translation elongation." Nature 440(7083): 561-564.

Fleischer, T. C., C. M. Weaver, et al. (2006). "Systematic identification and functional screens of uncharacterized proteins associated with eukaryotic ribosomal complexes." Genes Dev 20(10): 1294-1307.

Frischmeyer, P.A. (2002). An mRNA Surveillance Mechanism That Eliminates Transcripts Lacking Termination Codons. Science *295*, 2258–2261.

Garzia, A., Jafarnejad, S.M., Meyer, C., Chapat, C., Gogakos, T., Morozov, P., Amiri, M., Shapiro, M., Molina, H., Tuschl, T., et al. (2017). The E3 ubiquitin ligase and RNA-binding protein ZNF598 orchestrates ribosome quality control of premature polyadenylated mRNAs. Nature Communications *8*, 16056.

Guydosh, N.R., and Green, R. (2017). Translation of poly(A) tails leads to precise mRNA cleavage. RNA *23*, 749–761.

Guydosh, Nicholas R., and Rachel Green. “Translation of Poly(A) Tails Leads to Precise MRNA Cleavage.” RNA 23, no. 5 (May 2017): 749–61. https://doi.org/10.1261/rna.060418.116.

Harper, J. W. and E. J. Bennett (2016). "Proteome complexity and the forces that drive proteome imbalance." Nature 537(7620): 328-338.

He, F., and Jacobson, A. (2015). Nonsense-Mediated mRNA Decay: Degradation of Defective Transcripts Is Only Part of the Story. Annual Review of Genetics *49*, 339–366.

Higgins, R., Gendron, J.M., Rising, L., Mak, R., Webb, K., Kaiser, S.E., Zuzow, N., Riviere, P., Yang, B., Fenech, E., et al. (2015). The Unfolded Protein Response Triggers Site-Specific Regulatory Ubiquitylation of 40S Ribosomal Proteins. Molecular Cell *59*, 35–49.

Ito-Harashima, S., K. Kuroha, et al. (2007). "Translation of the poly(A) tail plays crucial roles in nonstop mRNA surveillance via translation repression and protein destabilization by proteasome in yeast." Genes Dev 21(5): 519-524.

Iuchi, S. (2001). Three classes of C2H2 zinc finger proteins. CMLS, Cell. Mol. Life Sci. *58*, 625–635.

Joazeiro, C.A.P. (2017). Ribosomal Stalling During Translation: Providing Substrates for Ribosome-Associated Protein Quality Control. Annual Review of Cell and Developmental Biology *33*, 343–368.

Juszkiewicz, S., and Hegde, R.S. (2017). Initiation of Quality Control during Poly(A) Translation Requires Site-Specific Ribosome Ubiquitination. Molecular Cell *65*, 743-750.e4.

Klauer, A. Alejandra, and Ambro van Hoof. "Degradation of MRNAs That Lack a Stop Codon: A Decade of Nonstop Progress." Wiley Interdisciplinary Reviews. RNA 3, no. 5 (2012): 649–60. https://doi.org/10.1002/wrna.1124.

Komander, D., and Rape, M. (2012). The Ubiquitin Code. Annual Review of Biochemistry *81*, 203–229.

Korolchuk, V.I., Menzies, F.M., and Rubinsztein, D.C. Mechanisms of cross-talk between the ubiquitin-proteasome and autophagy-lysosome systems. FEBS Letters *584*, 1393–1398.

Kuroha, K., Akamatsu, M., Dimitrova, L., Ito, T., Kato, Y., Shirahige, K., and Inada, T. (2010). Receptor for activated C kinase 1 stimulates nascent polypeptide-dependent translation arrest. EMBO Reports *11*, 956–961.

Liew, C.W., Sun, H., Hunter, T., and Day, C.L. (2010). RING DOMAIN DIMERIZATION IS ESSENTIAL FOR RNF4 FUNCTION. Biochem J *431*, 23–29.

Lykke-Andersen, J. and E. J. Bennett (2014). "Protecting the proteome: Eukaryotic cotranslational quality control pathways." J Cell Biol 204(4): 467-476.

Maquat, L.E., and Carmichael, G.G. (2001). Quality Control of mRNA Function. Cell *104*, 173–176.

Melnikov, S., A. Ben-Shem, et al. (2012). "One core, two shells: bacterial and eukaryotic ribosomes." Nat Struct Mol Biol 19(6): 560-567.

Metzger, M.B., Pruneda, J.N., Klevit, R.E., and Weissman, A.M. (2014). RING-type E3 ligases: Master manipulators of E2 ubiquitin-conjugating enzymes and ubiquitination. Biochimica et Biophysica Acta (BBA) - Molecular Cell Research *1843*, 47–60.

Meyuhas, O. (2015). "Ribosomal Protein S6 Phosphorylation: Four Decades of Research." Int Rev Cell Mol Biol 320: 41-73.

Mugnier, P., and Tuite, M.F. (1999). Translation Termination and Its Regulation in Eukaryotes: Recent Insights Provided by Studies in Yeast. *64*, 7.

Nakayama, K.I., and Nakayama, K. (2006). Ubiquitin ligases: cell-cycle control and cancer.

Nature Reviews Cancer *6*, 369–381.

Nicholson, P., and Mühlemann, O. (2010). Cutting the nonsense: the degradation of PTC-containing mRNAs. Biochemical Society Transactions *38*, 1615–1620.

Nilsson, J., Sengupta, J., Frank, J., and Nissen, P. (2004). Regulation of eukaryotic translation by the RACK1 protein: a platform for signalling molecules on the ribosome. EMBO Reports *5*, 1137–1141.

Ozsolak, F., Kapranov, P., Sylvain Foissac, Kim, S.W., Fishilevich, E., Monaghan, A.P., John, B., and Milos, P.M. (2010). Comprehensive Polyadenylation Site Maps in Yeast and Human Reveal Pervasive Alternative Polyadenylation. Cell *143*, 1018–1029.

Pena, C., E. Hurt, et al. (2017). "Eukaryotic ribosome assembly, transport and quality control." Nat Struct Mol Biol 24(9): 689-699.

Pisareva, V.P., Skabkin, M.A., Hellen, C.U.T., Pestova, T.V., and Pisarev, A.V. (2011). Dissociation by Pelota, Hbs1 and ABCE1 of mammalian vacant 80S ribosomes and stalled elongation complexes. EMBO J *30*, 1804–1817.

Richter, J. D. and J. Coller (2015). "Pausing on Polyribosomes: Make Way for Elongation in Translational Control." Cell 163(2): 292-300.

Samali, A., Fulda, S., Gorman, A.M., Hori, O., and Srinivasula, S.M. (2010). Cell Stress and Cell Death. Int J Cell Biol *2010*.

Schuller, A.P., and Green, R. (2018). Roadblocks and resolutions in eukaryotic translation. Nature Reviews Molecular Cell Biology.

Schulman, B.A., and Harper, J.W. (2009). Ubiquitin-like protein activation by E1 enzymes: the apex for downstream signalling pathways. Nat Rev Mol Cell Biol *10*, 319–331.

Shao, S., A. Brown, et al. (2015). "Structure and assembly pathway of the ribosome quality control complex." Mol Cell 57(3): 433-444.

Shoemaker, C.J., and Green, R. (2012). Translation drives mRNA quality control. Nat Struct Mol Biol *19*, 594–601.

Silva, G. M., D. Finley, et al. (2015). "K63 polyubiquitination is a new modulator of the oxidative stress response." Nat Struct Mol Biol 22(2): 116-123.

Simms, C. L., L. L. Yan, et al. (2017). "Ribosome Collision Is Critical for Quality Control during No-Go Decay." Mol Cell 68(2): 361-373 e365.

Simms, C.L., Thomas, E.N., and Zaher, H.S. (2017b). Ribosome-based quality control of mRNA and nascent peptides. Wiley Interdisciplinary Reviews: RNA *8*, e1366.

Simsek, D. and M. Barna (2017). "An emerging role for the ribosome as a nexus for post-translational modifications." Curr Opin Cell Biol 45: 92-101.

Simsek, D., G. C. Tiu, et al. (2017). "The Mammalian Ribo-interactome Reveals Ribosome Functional Diversity and Heterogeneity." Cell 169(6): 1051-1065 e1018.

Sitron, C.S., Park, J.H., and Brandman, O. (2017). Asc1, Hel2, and Slh1 couple translation arrest to nascent chain degradation. RNA *23*, 798–810.

Sundaramoorthy, E., Leonard, M., Mak, R., Liao, J., Fulzele, A., and Bennett, E.J. (2017). ZNF598 and RACK1 Regulate Mammalian Ribosome-Associated Quality Control Function by Mediating Regulatory 40S Ribosomal Ubiquitylation. Molecular Cell *65*, 751-760.e4.

Thompson, M.K., Rojas-Duran, M.F., Gangaramani, P., and Gilbert, W.V. (2016). The ribosomal protein Asc1/RACK1 is required for efficient translation of short mRNAs. ELife Sciences *5*, e11154.

Wilusz, J.E., and Wilusz, J. (2014). Nonsense-mediated RNA decay: at the 'cutting edge' of regulated snoRNA production. Genes Dev *28*, 2447–2449.

Ye, Y., and Rape, M. (2009). Building ubiquitin chains: E2 enzymes at work. Nat Rev Mol Cell Biol *10*, 755–764.